Universidade do Minho
Escola de Ciências

Marina Manuel Gonçalves Antunes

Characterization of the relationship between the GPCR Smoothened and the RNA-binding protein SMAUG in *Drosophila melanogaster*: regulation by HH signalling

maio de 2017

Characterization of the relationship between the GPCR Smoothened and the RNA-binding protein SMAUG in *Drosophila melanogaster*: regulation by HH signalling

Marina Antunes

UMinho | 2017

Universidade do Minho
Escola de Ciências

Marina Manuel Gonçalves Antunes

Characterization of the relationship between the GPCR Smoothened and the RNA-binding protein SMAUG in *Drosophila melanogaster*: regulation by HH signalling

Master's thesis

Master's in Molecular Genetics

Project carried out under supervision of

Professor Anne Plessis

and of

Professor Sandra Cristina Almeida Paiva

May, 2017

DECLARATION

Name: Marina Manuel Gonçalves Antunes

Electronic mail address: mm.tw_25@hotmail.com Telefone: 916335332

Bilhete de Identidade/Cartão de Cidadão: 14362852

Title of the dissertation: Characterization of the relationship between the GPCR Smoothened and the RNA-binding protein Smaug in *Drosophila melanogaster*: regulation by HH signalling

Supervisors:

Professor Anne Plessis

Professor Sandra Cristina Almeida Paiva

Year of conclusion: 2017

Master's in Molecular Genetics

DE ACORDO COM A LEGISLAÇÃO EM VIGOR, NÃO É PERMITIDA A REPRODUÇÃO DE QUALQUER PARTE DESTA TESE/TRABALHO.

Universidade do Minho, 25/05/2017

Assinatura:

Marina Manuel Gonçalves Antunes

Acknowledgements

I would like to express my gratitude toward Dr. Anne Plessis for providing me the opportunity to do my intership at the Institut Jacques Monod, as well as for the huge support, the honesty and the work she put into helping me complete this journey with success.

I would also like to thank all members of the team "Development, Signalisation and Traffic" directed by Anne Plessis at the Institut Jacques Monod (IJM): Matthieu SANIAL (ITA - IATOS), for is guidance and patience, as well as Isabelle BECAM (Research Engineer), Lucia BRUZZONE (PhD) and Camilla Argüelles (PhD) for guidance, support and encouragement. And of course to Lisa BARBUGLIO (Master's student) for her friendship and support. And, finally, to the whole team for the friendship, the funny parts, and for creating an amazing work environment that allowed me to learn so much.

I would also like to thank my co-supervisor at the University of Minho, Professor Sandra Paiva, contributing to the completion of this project by helping with everything necessary at my home university.

I. Abstract

The conserved Hedgehog signalling pathway is central to embryogenesis and adult tissue homeostasis in metazoans, e.g. *Drosophila melanogaster* and vertebrates. Hedgehog (HH) acts as a morphogen regulating different cell fates depending on its concentration. HH transduction cascade is tightly regulated, and deregulation of HH signalling activity accounts for congenital diseases, carcinogenesis, neurological disorders and cardiovascular pathologies in humans. SMO, an oncogene of the GPCR family, is paramount to the transduction of the HH signal. In response to HH reception, SMO undergoes extensive phosphorylation, which controls its trafficking, leading to its accumulation at the plasma membrane in drosophila and in the primary cilium in vertebrates.

By proteomic and genetic screens, the team "Development, Signalisation and Traffic" directed by Anne Plessis at the Institut Jacques Monod (IJM) identified a novel partner of SMO: the RNA binding protein SMAUG. SMAUG is a key component of mRNA storage bodies where it controls the degradation and translation of many mRNA during fly embryonic development. Their data indicated SMAUG may both act as a positive regulator of HH signaling and be regulated by HH signaling. My goals were (i) to further characterize the interaction between SMO and Smaug, (ii) to analyze their colocalisation in fly cells (iii) to understand better its potential role in HH signaling during wing morphogenesis. Using a combination of molecular, cellular and genetic approaches, I (i) confirmed the colocalisation of SMO and SMAUG, and showed that it was due to their direct interaction, (ii) analyzed the implication of known phosphosites of SMO in the regulation of its interaction with SMAUG, and initiated the search for the kinases that were involved in the regulation of SMO/SMAUG interaction. Finally, my *in vivo* studies on the role of SMAUG revealed a synthetic lethal interaction with a mutant affecting HH signaling but the interpretation of their results remains unclear.

Altogether my data have brought novel information on this unexpected relationship which shed novel light on the function and regulation of both SMO and SMAUG.

Keywords: Smoothened, Hedgehog signalling, Smaug, signal transduction, *Drosophila melanogaster*

II. Resumo

A conservada via de sinalização Hedgehog (HH) é central durante embriogéneses e homeostasia do tecido adulto em metazoários, e.g. *Drosophila melanogaster* e vertebrados. HH atua como um fator morfogénico, regulando diferentes destinos celulares, o que depende da sua concentração. A cascata de tradução de HH é fortemente regulada e, desregulação da atividade de sinalização de HH é responsável por doenças congénitas, carcinogénese, desordens neurológicas e patologias cardiovasculares em humanos. Smoothened (SMO), um oncogene da família dos recetores acoplados a proteínas G, é fundamental para a transdução do sinal da via HH. Em resposta à receção de HH, SMO é extensivamente fosforilado, o que controla o seu tráfego, levando à sua acumulação na membrana plasmática em drosófila, e no cílio primário em vertebrados. Através the análises proteómicas e genéticas, a equipa de investigação "Desenvolvimento, Sinalização e Tráfego" dirigida por Anne Plessis no Instituto Jacques Monod (IJM) identificou um novo parceiro de SMO: uma proteína de ligação ao ácido ribonucleico (ARN), Smaug. Smaug é um componente crucial dos corpos de armazenamento de ARN mensageiro (ARNm) onde controla a degradação e a tradução de muitos ARNm durante o desenvolvimento embrionário na mosca. Os dados obtidos pela equipa indicam que SMAUG possa atuar como regulador positivo da sinalização da via HH, e ser regulado pela mesma via. Os meus objetivos foram (i) caraterizar em maior detalhe a interação entre SMO e SMAUG, (ii) analisar a co localização entre as duas proteínas em células de mosca derivadas do disco imaginário da asa (estrutura que dá origem à asa adulta), (iii) de forma a compreender melhor o potencial papel da relação entre as duas proteínas durante a morfogénese da asa. Através da combinação de técnicas moleculares, celulares e genéticas, eu (i) confirmei a co localização de SMO com SMAUG, e mostrei que esta co localização é devida à interação direta entre as duas proteínas, (ii) analisei a implicação de sítios de fosforilação em SMO, descritos na literatura, na regulação da interação de SMO com SMAUG, e iniciei a procura pelas cinases que estão envolvidas na regulação da interação SMO/SMAUG. Finalmente, os meus estudos *in vivo* sobre o papel de SMAUG revelaram uma interação sintática letal com uma mutação que afeta a via de sinalização de HH. Contudo, a interpretação destes resultados permanece pouco clara. Em conjunto, os meus dados trouxeram informação adicional sobre esta relação inesperada, contribuindo para a compreensão da função e regulação de ambos SMO and SMAUG.

Palavras-chave: Smoothened, via de sinalização Hedgehog, transdução de sinal, SMAUG, *Drosophila melanogaster*

TABLE OF CONTENTS

I. Abstract iv

II. Resumo v

III. List of abbreviations and acronyms x

IV. LIST OF FIGURES xii

V. LIST OF TABLES xiii

VI. Introduction 1

A. Drosophila melanogaster as a model organism for research 1

B. The roles of the HH signalling pathway 2

1. In drosophila 2

2. In vertebrates 3

C. The HH signalling pathway: transduction through the GPCR SMO 4

1. General mechanisms in drosophila 4

2. General mechanisms in mammals 5

D. The GPCR SMO 7

1. SMO structure 7

2. SMO phosphorylation, conformational switch and activation in response to HH gradient 8

3. SMO trafficking and cell surface expression: phosphorylation-regulated ubiquitination 13

4. The role of sumoylation of SMO in its activity 14

5. The role of lipids in the regulation of SMO activity 15

6. Recruitment and activation of intracellular signalling multiprotein complexes by activated SMO 16

E. The RNA-binding protein SMAUG 18

F. Main aims of my project....20
VII. Materials and methods....21
A. Drosophila experiments....21
1. Fly stocks and Crosses....21
2. Wing imaginal disc immunostaining....23
3. Fly wing....24
4. Statistics....24
B. Cloning procedures....24
1. By restriction enzyme-ligation procedures....25
2. By the Gateway technology....25
3. Chemo-transformation:....26
4. Clones selection and validation....27
C. SMO constructs....28
D. RNA interference (RNAi)....30
E. Cell culture and Transfection....31
F. Cell extraction, Western Blotting and immunostaining....32
G. Immunoprecipitation for Co-IP assay using magnetic separation....33
H. Cell fixation for fluorescent cell imaging....34
VIII. Results....35
A. SMO and SMAUG co-localise in co-transfected CI8 cells, with or without HH, in an interaction-dependent manner....35
1. Choice of the fluorescent tag....35
2. SMO and SMAUG co-localise in CI8 cells with and without HH....35
3. SMO and SMAUG interaction is required for their co-localisation....37
B. SMO interacts with SMAUG in a phosphorylation-dependent manner....38
1. Identification of the phosphosites of SMO which phosphorylation prevents interaction with SMAUG....40

2. Identification the kinase responsible for the phosphorylation that prevents SMO interaction with SMAUG 46

C. Exploring the role of SMAUG in the HH signalling pathway 47

1. SMAUG loss or depletion has no obvious effect on HH signalling in a wild type background 48

2. SMAUG depletion seems to enhance the patterning defects caused by *fu* loss-of-function 48

3. Fu knockout 51

IX. Discussion 51

X. Bibliography 57

III. List of abbreviations and acronyms

A	Anterior
A/P	Anterior/Posterior
aPKC	Atypical protein kinase C
anti-SmoP	Smo phospho-specific antibody
Bud	Budesonide
CD	Cytoplasmic domain
CK1	Casein kinase 1
CK2	Casein kinase 2
Ci	Cubitus interruptus
Ci^{A}	Ci activator form
Ci^{F}	Full-length Ci
Ci^{R}	Truncated Ci repressor form
col	*collier*
Cos2	Costal2
CRD	Cysteine-rich domain
C-tail	Carboxyl-terminal intracellular tail
DB	Disulphide bridges
DHH	Desert hedgehog
dpp	*decapentaplegic*
ECD	Extracellular domain
ECL	Extracellular loop
ECLD	Extracellular linker domain
en	*engrailed*
Fu	Fused
gish	*gilgamesh*
Gli	Glioma-associated oncogene
Gli^{A}	Gli activator
GP	G protein
GPCR	G protein-coupled receptor
Gprk2	G protein-coupled receptor kinase 2
GSK3	Glycogen synthase kinase 3

HH	Hedgehog
ICL	Intracellular loop
IHH	Indian hedgehog
Ihog	Interference hedgehog
NMR	Nuclear magnetic resonance
P	Posterior
PI(4)P	Phosphatidylinositol 4-phosphate
PKA	Protein kinase A
PP2A	Protein phosphatase 2A
PP4	Protein phosphatase 4
Ptc	Patched
Sac1	Sac1 lipid phosphatase
Ser/Thr	Serine/Threonine
SHH	Sonic hedgehog
SMO	Smoothened
Stt4	Stt4 phosphatidylinositol 4-kinase
Su(fu)	Suppressor of fused
7TM	Heptahelical transmembrane
TF	Transcription factor
USP8	Ubiquitin-specific protease 8
wg	*wingless*

IV. LIST OF FIGURES

Figure 1: The D. melanogaster's life cycle. 1

Figure 2: The wing imaginal disc and the adult wing as platforms for the study of the HH pathway. 3

Figure 3: The HH signalling pathway in Drosophila and mammals. 6

Figure 4: Structure of human SMO. 7

Figure 5: SMO conformational switch in response to HH. 10

Figure 6: GISH and CK1γ localise to the plasma membrane and to the primary cilium, respectively. 12

Figure 7: Model of regulation of SMO by HH-dependent sumoylation. 14

Figure 8: PI(4)P regulates Smo phosphorylation and membrane (left)/ciliary (right) accumulation. 15

Figure 9: Model of how SMO/FU interact to promote high-throughput HH signalling. 17

Figure 10: Action mechanisms of SMAUG. 19

Figure 11: The Gal4/UAS system. 22

Figure 12: Gateway site-specific recombination system. 26

Figure 13: Mechanism of action of shRNA-plasmid gene silencer. 31

Figure 14: Subcellular distribution of SMO-mCherry and GFP-SMAUG in presence or absence of HH. 36

Figure 15: Subcellular distribution of SMOΔ958-mCherry, SMOΔ1004-mCherry and GFP-SMAUG in presence or absence of HH. 38

Figure 16: SMO and SMAUG co-immunoprecipitate in absence and presence of HH, however the interaction is lost when SMO is hyperphosphorylated in presence of HH. 39

Figure 17: Co-IP of SMO 5S/TA-HA with Myc-SMAUG in presence and absence of HH 41

Figure 18: Co-IP of SMO c14A-HA with Myc-SMAUG in presence and absence of HH 43

Figure 19: Expression of several Myc-SMO mutants in presence and absence of HH. 45

Figure 20: Validation of shRNA targeting specific kinases. 47

Figure 21: Genetic interaction between the Fu1 mutant and the decrease in SMAUG activity. 50

Figure 22: Model of the regulation of SMO/SMAUG interaction in presence and absence of HH 56

V. LIST OF TABLES

Table 1: Fly lines. 21

Table 2: smo mutant constructs used to transfect CI8 cells for Western Blotting or Co-IP experiments. Ser and Thr of smo C-terminal tail coding sequence have been mutated to either Alanine (⟶ A) or Aspartic acid (⟶ D). All plasmids contain a marker gene. 29

Table 3: Other constructs used to transfect CI8 cells for Western Blotting or Co-IP experiments. All plasmids contain a marker gene of resistance to ampicillin. 30

Table 4: Plasmid constructs used to transfect CI8 cells for fluorescent cell imaging studies. All plasmids contain a marker gene of resistance to ampicillin. 30

VI. Introduction

A. Drosophila melanogaster as a model organism for research

The discovery of the *white* mutation and its linkage to the X-chromosome by T.H. Morgan popularised the use of drosophila as a model organism for research in the genetics field. Nowadays, the fruit fly is extensively used for that purpose. Among the advantages of this model are i) husbandry: flies are easy and cheap to maintain, even hundreds of stocks at time; ii) their life cycle is around 10 days (Fig. 1), which means that successive generations with large progeny can be obtained quite quickly ; iii) the availability of sophisticated methods for forward genetics, with the possibility to carry out unbiased genome screens, but also to produce and study mosaic clones; iv) their genome is sequenced and here there is little redundancy among the different genes, which is very helpful in reverse genetics; (v) numerous strategies and techniques have been developed that allow to manipulate drosophila genes for reverse genetics; vi) the small size and complexity of their tissues and organs, makes it easy to manipulate them experimentally; vii) there are comprehensible databases with the hundreds of fly lines available for research, as well as extensive knowledge on this organism; viii) finally, many biological processes, including complex ones, are conserved from drosophila to humans (reviewed in Roote, J., & Prokop, A. 2013)

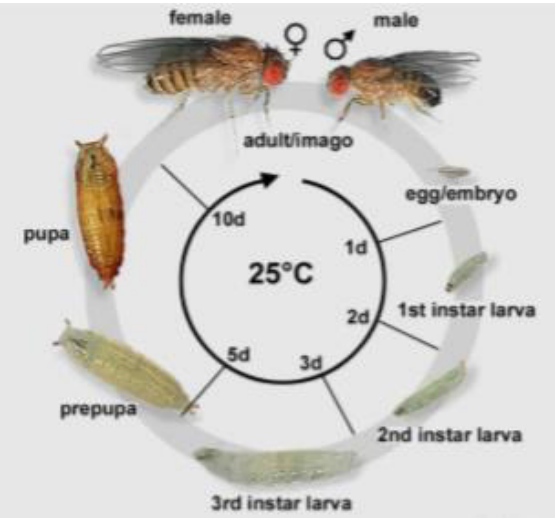

Figure 1: The D. melanogaster's life cycle.

At 25 °C, after egg laying, the embryo phase lasts ~21 hours, and ~1 day is required between each larval stage. 1 day into the 3d instar stage, larvae leave the medium and start wandering

on the tube walls; eventually, they pupariate. During pupal stages, organ degeneration (histolysis) and restructuration (metamorphosis) occurs. ~5 days later, flies hatch (eclosure). At this point, males take up 8 hours to mature sexually. At 18 °C, each chronological event takes double the time to occur (Roote, J., & Prokop, A., 2013).

In light of all the advantages mentioned, and in particular, the last one: conservation, it is not surprising that drosophila is widely employed for the study of the Hedgehog (HH) pathway, which was described for the first time in the fruit fly, and on which this project is based.

B. The roles of the HH signalling pathway

From drosophila to humans, the HH transduction cascade controls patterning and growth during the development of many metazoans. It controls cell fate, i.e. differentiation, migration, death and proliferation, during numerous developmental processes.

1. In drosophila

In the fly model, it controls the development of the many structures such as wing, eye and leg (Ingham et al. 2011; Ingham et al. 2001; Jiang & Hui 2008). In fact, one widely used and well-characterised structure to study the HH pathway experimentally is the structure that gives rise to the fly's adult wing: the wing imaginal disc (WID). In this epithelial structure, an HH gradient is established in the cells of the anterior (A) compartment due to its production and secretion by the cells of the posterior (P) compartment, and its subsequent diffusion through the A/P boundary. HH triggers, in a concentration-dependent manner, the expression of genes such as *iroquois* (*iro*), *decapentaplegic* (*dpp*), *engrailed* (*en*), *collier* (*col*) and *patched* (*ptc*), which are pivotal to A/P patterning of the *Drosophila*'s wing (Vervoort et al. 1999; Strigini & Cohen 1997; Basler & Struhl 1994; Tabata & Kornberg 1994). In other words, the HH gradient is translated into the expression of different genes, e.g. *iro* and *dpp* are responsive to low, *ptc* to intermediate and *en* to peak levels of HH (Fig.2) (Strigini & Cohen 1997). Thus, the determination of the level and pattern of expression of these target genes, in the wing imaginal disc, allows to monitor the extent of HH signalling activity (Fan et al. 2012).

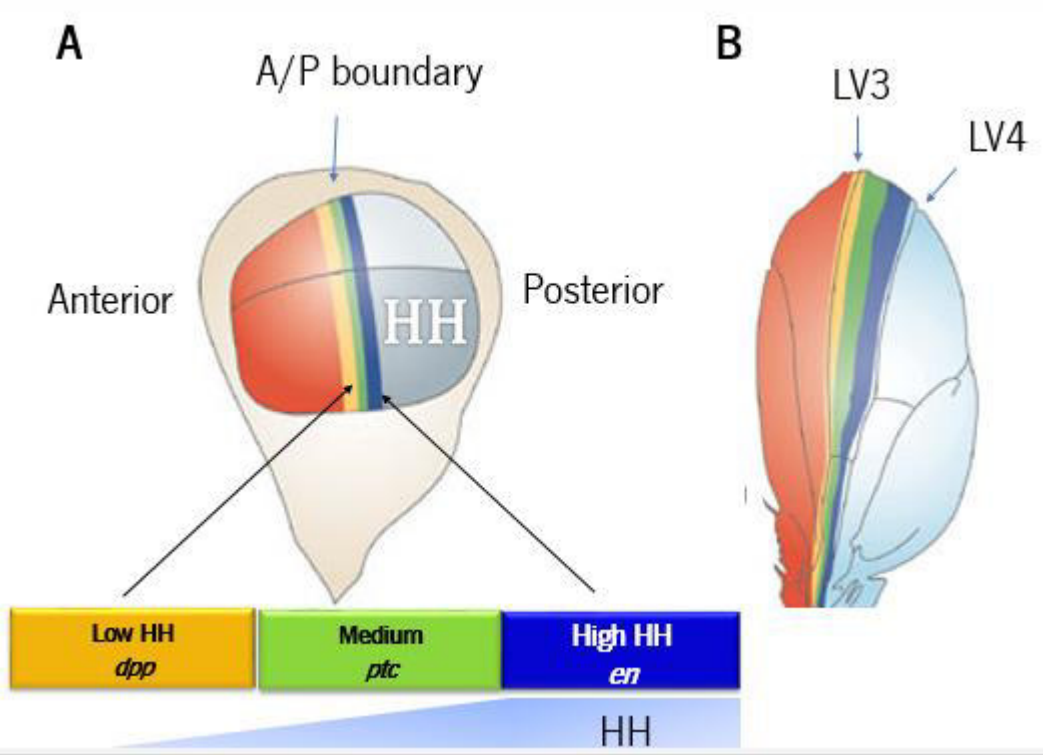

Figure 2: The wing imaginal disc and the adult wing as platforms for the study of the HH pathway.

(A, B) The wing imaginal disc develops into the adult wing through processes of morphogenesis and growth that are dependent on HH. HH is produces in the cells of the posterior compartment, and diffuses to ~12 rows of anterior compartment cells juxtaposed to the A/P boundary. According to the amount of HH with which the cells are in contact, different genes will be expressed. These genes are involved in the wing blade growth and/or the patterning of longitudinal vein (LV) 3 and 4 according to the colour code: low, medium and high HH levels promote dpp, ptc and en expression, respectively. (Hartl & Scott 2014).

2. In vertebrates

In vertebrate's development, HH proteins also play important roles. For instance it allows the antero-posterior polarisation of the limb bud, or the dorso-ventral polarisation of the nervous system. Deregulation of this signalling pathway during development leads to birth defects and congenital disorders (Jiang & Hui 2008; Pasca di Magliano & Hebrok 2003; Briscoe1 et al. 2013; Petrova & Joyner 2014; Ingham et al. 2001; Taipale & Beachy 2001). Past embryogenesis, the HH signalling pathway has a critical role in adult tissue homeostasis of mammalian organisms. It ensure the repair of ischemic tissues and seems to have a protective role against neuro and

muscular degeneration. However, deregulation of HH signalling has been associated to numerous cancers e.g. basal cell carcinoma, breast cancer, lung cancer, etc. Point mutations in genes that encode key proteins of this signalling cascade have been shown to promote tumours, and the expression of HH in the tumour or stroma cells favours the progression of numerous cancers (Paslay et al. 2010),(Jiang & Jia 2015). The therapeutic targeting of the proteins of the HH transduction cascade is, thus, considered as crucial for the treatment of these pathologies (Jiang & Hui 2008; Pasca di Magliano & Hebrok 2003; Briscoe1 et al. 2013; Petrova & Joyner 2014; Ingham et al. 2001; Taipale & Beachy 2001).

C. The HH signalling pathway: transduction through the GPCR SMO

1. General mechanisms in drosophila

The seven transmembrane receptor Smoothened (SMO), on which my project is focused, is necessary for HH signal transduction, and some mutations in SMO have been shown to have oncogenic effects (Paslay et al. 2010), (Jiang & Jia 2015).

In the absence of the HH signal, the twelve-transmembrane receptor Patched (PTC) accumulates at the cell surface, and exerts an inhibitory effect over SMO, preventing its activation and, consequently, signal transduction. This inactivation of SMO is associated to its internalisation in intracellular compartments, leading to its degradation in the lysosome. This results in the cleavage of a Zinc finger transcription factor called Cubitus interruptus (CI) into a repressor form that prevents the expression of its target genes. Binding of HH to PTC promotes lifting of the inhibition PTC exerts on SMO, and also leads to the internalisation of PTC/HH complex, and to the accumulation of a hyperphosphorylated, form of SMO at the plasma membrane. This leads, via the interaction of SMO with cytosolic proteins, to the inhibition of CI processing, enabling the full-length CI to enter the nucleus and promote expression of its target genes (Fig. 3 A).

In what way PTC inhibits SMO, and how HH counteracts this inhibition has been a longstanding question. Some recent studies on phosphatidylinositol-4-phosphote (PI(4)P), and how it promotes SMO phosphorylation and conformational change through interaction with its C-tail, appear to have added one more piece to the puzzle (Jiang et al. 2016).

2. General mechanisms in mammals

SMO, PTC and most members of the HH pathway are conserved in vertebrates, Moreover, vertebrates have three HH ligands: SHH, IHH and DHH, two patched receptors (PTC1 and 2), and three CI related transcription factors called Gli 1, 2 and 3 (Arensdorf et al. 2016).

However, one important difference is the requirement of the primary cilium for signal transduction, a structure that is absent in most fly cells for HH signalling (Kuzhandaivel et al. 2014) (Kuzhandaivel et al. 2014). In absence of HH, PTC concentrates in the cilium and prevents SMO accumulation in this structure. Binding of HH to PTC, leads to the receptor's endocytosis, followed by SMO accumulation in the cilium, where it is phosphorylated, dimerised and activated, leading to target gene expression by activated Gli (Gli A) (Fig. 3 B).

In addition to the canonical signalling cascade, which leads to SMO-dependent Gli activation, vertebrates are also able to activate a non-canonical pathway that, through Gαi, regulates metabolism, proliferation, Ca^{+2} flux, etc. Non-canonical HH signalling pathways may also be in the origin of emerging resistance to drugs that target SMO for the treatment of cancer, such as pancreatic cancer.

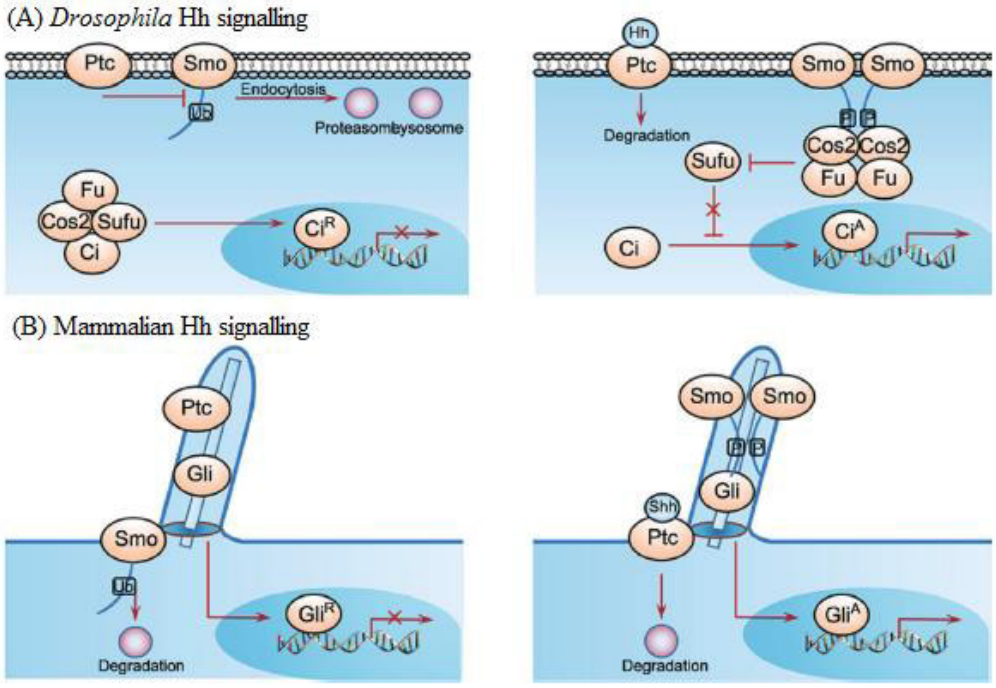

Figure 3: The HH signalling pathway in Drosophila and mammals.

(A) In Drosophila, in the absence of HH (left panel), the C-tail of PTC-inhibited SMO, which undergoes ubiquitination, which leads to SMO internalisation and subsequent lysosomal and proteasomal degradation. The transcription of HH target genes is blocked by CIR, the product of CIF proteolytic cleavage. The binding of HH to PTC (right panel), suppresses SMO inhibition and promotes its phosphorylation. SMO accumulates at the plasma membrane, dimerises and becomes active, enabling CIA to enter the nucleus and trigger transcription. (B) In mammals, in the absence of HH (left panel), the presence of PTC in the primary cilium stops SMO accumulation into the organelle and inhibits the signalling pathway. Binding of HH to PTC (right panel) leads to the receptor's endocytosis, followed by SMO accumulation in the cilium, where it is phosphorylated, dimerised and activated. Target gene expression is triggered by GLIA (Jiang & Jia 2015).

D. The GPCR SMO

1. SMO structure

The protein SMO belongs to the Frizzled family of GPCRs (Fig. 4). The amino acid sequence of SMO is arranged in three distinct domains: extracellular (ECD), the heptahelical transmembrane (7TM) and cytoplasmic (CD) (Fredriksson et al. 2003).

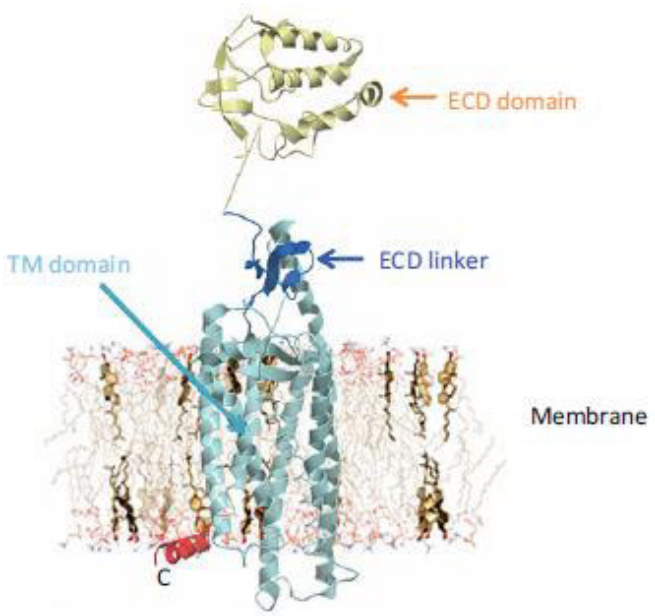

Figure 4: Structure of human SMO.

ECD and TM X-ray structures exhibited. Besides the initial α-helix, CD structure has yet to be completely unravelled (Paslay et al. 2010).

The ECD possesses a highly conserved cysteine-rich domain (CRD) and a linker domain (ECLD) at its N-terminal. In humans, the cysteines establish four disulphide bridges (DBs) that,

alongside the hydrogen-bonding network, secure the connection of three extracellular loops (ECLs) to the linker domain (Paslay et al. 2010).

In drosophila, besides the eight cysteines of CRD, which establish four DBs, the ECLD also has five conserved cysteines that stabilise SMO conformation. Individual mutations of the CRD cysteines to alanine have shown that C90-C155 and C139-C179 are central to the maintenance of the domain's integrity and downstream signalling, since the mutants in which these DBs did not form were incapable of rescuing HH-induced reporter gene in a *smo*-knockdown background (Rana et al. 2013). ECD may be responsible for SMO dimerization in drosophila since, in previous studies using mutants in which this domain had been deleted, the transducer did not dimerise and was inactive (Rana et al. 2013), (Zhao et al. 2007). In vertebrates, ECD deletion does lead to inactive SMO, however HH signalling is reduced, and there is an increase of SMO accumulation at the cilium base and of basal activity. The latter is supressed by PTC, which seems to indicate that SMO inhibition by the HH receptor does not necessarily depend on ECD (Paslay et al. 2010).

Three ECLs and three ICLs connect the helices of the 7 TM domain. TM and ECD have well-described ligand binding-pockets (reviewed in (Paslay et al. 2010)). The drosophila SMO may have an allosteric site for an endogenous modulator at the CRD, since the latter is able to bind the glucocorticoid budesonide (Bud). Rana and colleagues speculate the binding of this endogenous activator could trigger the SMO conformational switch. Bud also binds to human SMO CRD, albeit more strongly than in drosophila's case (Rana et al. 2013).

The CD mediates SMO phosphorylation by multiple kinases, e.g. G protein coupled receptor kinase 2 (GRK2), in the presence of HH (Paslay et al. 2010).

2. SMO phosphorylation, conformational switch and activation in response to HH gradient

It has been established through immune-purification and mass spectrometry techniques that, in drosophila, HH promotes the phosphorylation of SMO C-tail at more than 26 Serine/Threonine (Ser/Thr) (Zhang et al. 2004). This involves many kinases such as the c-AMP-dependent protein kinase A (PKA), casein kinase 1 (CK1) - mainly the isoforms CK1α/ε - casein kinase 2 (CK2), atypical protein kinase C (aPKC), GprK2 and Fused (FU) (Jiang et al. 2014)(Maier et al. 2014) (Fan et al. 2012), (Sanial et al. 2017).

a) PKA/CK1-mediated phosphorylation

In the presence of HH, PKA and CK1 sequentially phosphorylate SMO C-tail at three membrane-distal clusters of Ser/Thr residues (Fig.5 A). This phosphorylation is essential to switch from inactive to active SMO. In absence of HH, the SMO is dephosphorylated due to the action of the phosphatase PP2A (Jia et al. 2009), and is under a closed, inactive conformation due to intramolecular interactions between two regions of its C-tail: an arginine rich region imbedded in the PKA/CKI clusters, and an acidic region in the most terminal region. Moreover, this form is ubiquitinated, which promotes its internalization and degradation (Xia et al. 2012)

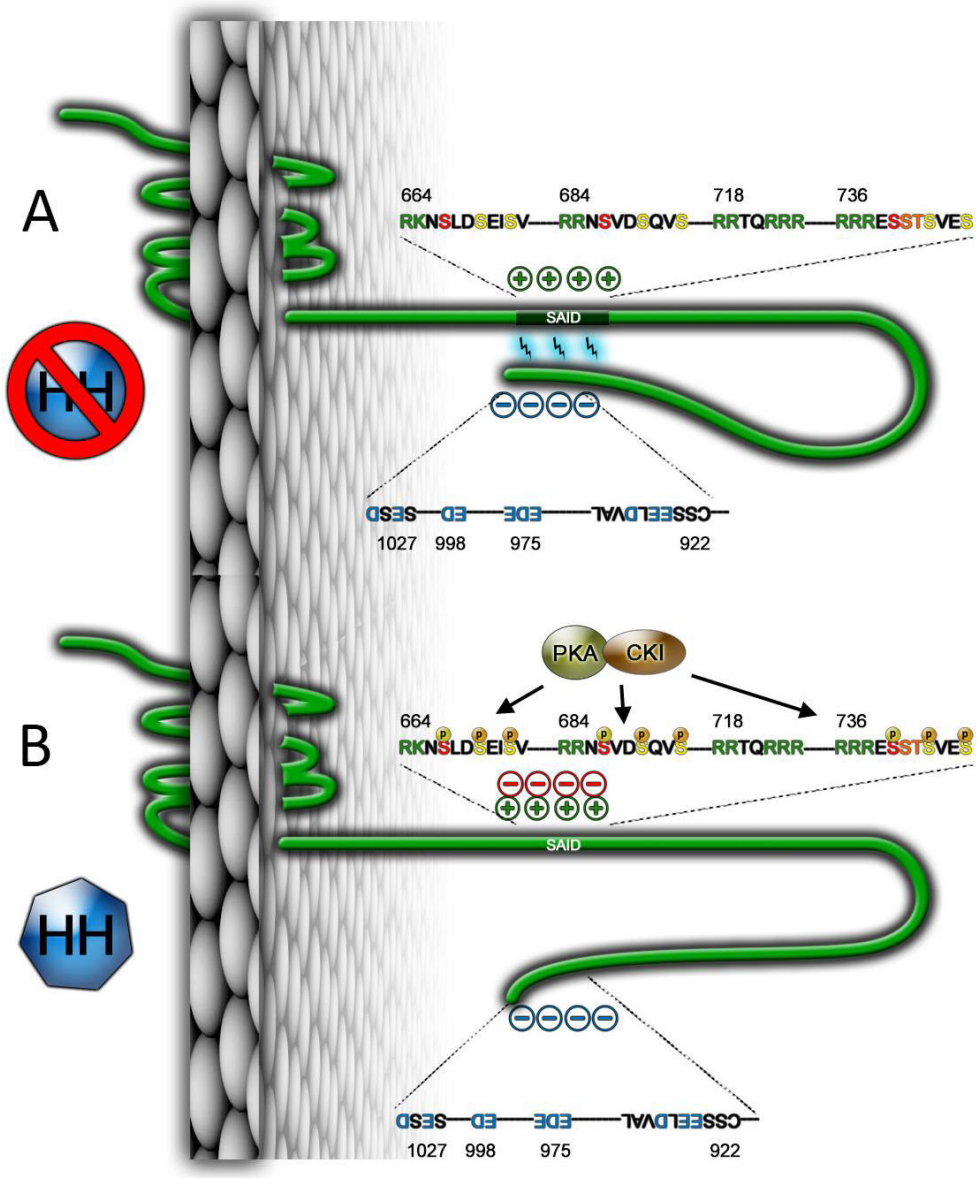

Figure 5: SMO conformational switch in response to HH.

(A) In absence of HH, the arginine (R) clusters (SAID domain), which are positively charged, establish electrostatic bonds with the negatively charged residues in the C-terminus. (B) In presence of HH, the negative charges of the phosphate groups added to the C-tail by PKA/CK1,

neutralise the positive charges in the SAID domain. The electrostatic bonds disappear and SMO undergoes a conformational switch. Adapted by M. Sanial after (Zhao et al. 2007).

The phosphorylation of the PKA/CKI sites, induced by HH, introduces negative charges (due to the phosphate groups). It induces an open conformation by neutralizing the positive charges of the adjacent arginines and thus disrupting their interaction with the negatively charged C-terminal region. This allows dimerization of SMO C-tail (Fig. 5B) (Zhao et al. 2007). Based on biochemical and Fluorescence Resonance Energy Transfer (FRET) experiments, Fan and colleagues proposed a "zipper-lock model" where the gradual phosphorylation of PKA and CK1 sites, due to the HH gradient, induces a gradual conformational change in SMO C-tail. Moreover, the PKA/CK1-mediated phosphorylation of SMO also prevents its ubiquitination. This prevents its internalisation and leads to its accumulation at the cell surface (Fan et al. 2012). Although phosphorylation is clearly required for its activation and function, phosphomimetic mutations indicate the post-translational modification is not sufficient to promote full-fledge SMO activation, which is possibly, influenced by other mechanisms in parallel to phosphorylation (Fan et al. 2012).

b) Gprk2-mediated phosphorylation

GPCR proteins are often regulated by a class of kinases called the GPRK and it was shown that in fly, Gprk2 contributes to SMO activation by several means. Firstly, it forms a dimer/oligomer that binds to the SMO C-tail and induces, in a kinase-independent manner, SMO dimerization and activation. Secondly, Gprk2 directly phosphorylates C-tail of SMO (at S 741/Thr742). This latter effect is favoured by PKA and CK1 phosphorylation at the adjacent S residues (Chen et al. 2010), and greatly enhance SMO.

c) Gilgamesh-mediated phosphorylation

Gilgamesh (*GISH),* a protein kinase that belongs to the Casein Kinase 1 γ family was identified thanks to a genetic modifier screen as a positive regulator of SMO (Hummel et al. 2002; Knippschild et al. 2005). In response to high levels of HH, membrane tethered GISH can phosphorylates SMO on a S/T cluster in the juxtamembrane region of SMO cyto-tail (Fig. 6) (Gault et al. 2012; Davidson et al. 2005) (Li et al. 2016). In mammals, GISH is located in the primary cilium and also acts on SMO to enhance its activation.

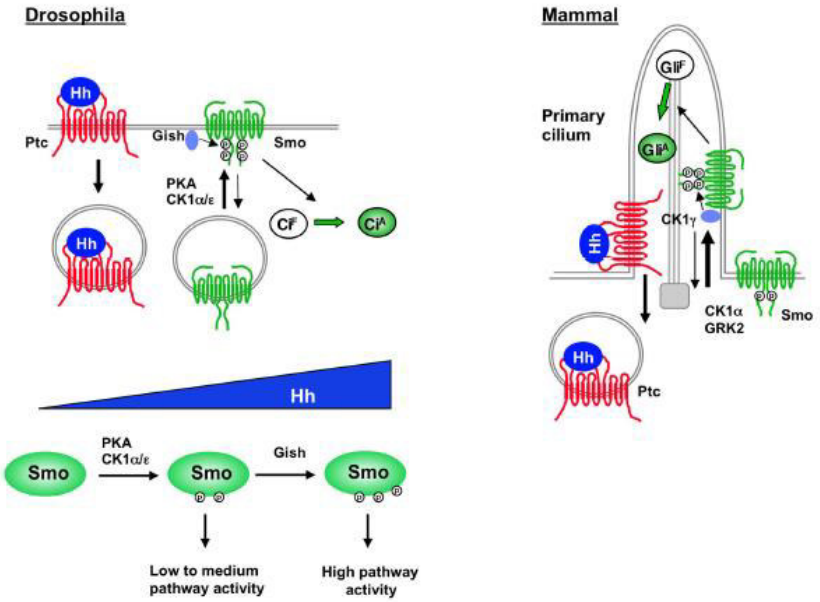

Figure 6: GISH and CK1γ localise to the plasma membrane and to the primary cilium, respectively.

In drosophila (left) and mammals (right), these kinases modulate the HH signalling pathway through the phosphorylation of SMO. In the presence of HH, SMO accumulates to the membrane/cilium, where it associates with, is phosphorylated and activated by GISH/CK1γ. In Drosophila, HH gradient promotes differential SMO phosphorylation by PKA/CK1 and GISH, which ultimately translates into differential levels of HH signalling pathway activity (Li et al. 2016).

d) aPKC-mediated phosphorylation

Besides its role in regulating cell polarity, the atypical protein kinase C (aPKC) has an important, conserved role in the HH signalling pathway. In *Drosophila*, it contributes to signal transduction and HH targeted gene expression by phosphorylating SMO (at its Ser680 residue). SMO phosphorylation by aPKC leads to its basolateral accumulation (Jiang et al. 2014).

e) Fu-mediated phosphorylation

Finally, a studies from my lab, revealed that a protein kinase called Fused (FU) could bind to the most C-terminal part of SMO C-tail and phosphorylates 4 adjacent clusters of S/T residues (Liu et al. 2007), (Chen & Jiang 2013). This phosphorylation greatly contributes to SMO full-

blown activation. The interaction of SMO/FU is, however, complex and will be explored in more detail ahead (Sanial et al. 2017).

f) SMO phosphorylation in mammals

Mammalian SMO does not have the three PKA/CK1 phosphorylation clusters that exist in the fly. Rather, it is activated by CK1α and GRK2-dependent phosphorylation in its C-tail which also promotes its localization to the primary cilium (Chen et al. 2010).

CK1γ is the Gilsh orthologue in vertebrates (Hummel et al. 2002; Knippschild et al. 2005). There are three isoforms of CK1γ, all encoded by different genes. The C-terminal of CK1γ also undergoes palmitoylation to localise to the primary cilium as it does for its plasma membrane localisation in fly (Gault et al. 2012; Davidson et al. 2005). Here, as in the fly, CK1γ role is to enhance SMO activity and, consequently, boost HH signal transduction.

Contrary to its importance for the HH pathway in drosophila, FU appears to have no role in vertebrates HH pathway.

3. SMO trafficking and cell surface expression: phosphorylation-regulated ubiquitination

Ubiquitination exerts its negative role on HH signalling activity by regulating the internalization and degradation of HH pathway components such as PTC and SMO. Thus, SMO undergoes both mono- and poly-ubiquitination and, as a result, after endocytosis, is targeted to the lysosome for degradation. An *in vivo* RNAi screen, allowed Xia et al. (2012) to identify the deubiquitinase USP8 that functions as an HH signalling positive regulator. USP8 acts by reducing SMO ubiquitination levels, preventing its localization to early endosomes, and promoting its cell surface accumulation. UPS8 interacts with the amino acids 625-753 of SMO, a region that covers the PKA/CK1 phosphorylation clusters.

USP8 knockout promotes a decrease in SMO accumulation and therefore of HH signalling activity due to the increase in SMO ubiquitination. On the contrary, USP8 overexpression augments signalling activity by precluding SMO ubiquitination and increasing SMO accumulation. Notably PTC is able to inhibit the SMO accumulation induced by USP8 overexpression. Similarly, inactivation of Uba1, an ubiquitin activating enzyme, induces SMO cell surface accumulation and signal activation. (Xia et al. 2012; Li et al. 2012). In response to HH, the inhibition of SMO

ubiquitination by the PKA-CK1-mediated phosphorylation of its C-tail leads to accumulation at the plasma membrane.

Despite the well-known role of ubiquitination in modulating SMO activity, the E3 ligases that interact with SMO have yet to be identified (Hsia et al. 2015).

4. The role of sumoylation of SMO in its activity

A recent study provided more information on the dynamics of SMO trafficking, particularly on its regulation by sumoylation and ubiquitination. It shows that HH promotes the sumoylation of SMO C-tail at lysine (K) 851, which in turn favours SMO accumulation at the plasma membrane by antagonising its ubiquitination (Fig. 7). In contrast, in absence of HH, the interaction between *Ulp1* and SMO, which is favoured by Krz (the drosophila β-arrestin 2), leads to SMO desumoylation and ubiquitination. Interestingly, sumoylation of SMO seems to occur in a PKA/CK1 phosphorylation-independent manner, since both phosphodeficient and phosphomimetic forms of SMO for PKA/CK1 clusters were equally sumoylated (Ma et al. 2016),(Zhang et al. 2017).

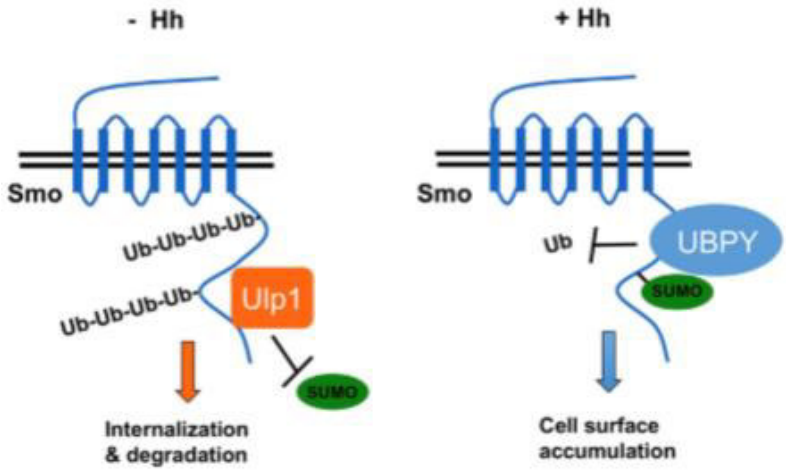

Figure 7: Model of regulation of SMO by HH-dependent sumoylation.

(Left) In absence of HH the Ubiquitin-like protease (Ulp1) prevents SMO C-tail sumoylation and promotes its ubiquitination. As a result, SMO is endocytosed and degraded. (Right) On the other hand, HH promotes SMO C-tail sumoylation. The SUMO molecules anchored to the C-tail recruit UBPY, which in turn antagonises ubiquitination and, as a consequence, promotes SMO cell surface accumulation (Ma et al. 2016).

5. The role of lipids in the regulation of SMO activity

In what way PTC inhibits SMO and how HH counteracts this inhibition is a longstanding question. However, some recent studies on phosphatidylinositol-4-phosphote (PI(4)P) and how it promotes Smo phosphorylation and conformational change through interaction with its C-tail appear to have added one more piece to the puzzle (Jiang et al. 2016). Using drosophila wing discs and cultured cells, Jiang et al (2016) demonstrated that, under HH stimulation, PI(4)P is able to induce the transducer's phosphorylation, conformational change and activation via its interaction with an arginine motif in SMO C-tail while low PI(4)P levels repress signalling activity in the absence of HH. Furthermore, it was found that GRK2 augments PI(4)P levels. A pleckstrin homology (PH) domain in GRK2 mediates its kinase-independent activity. In other words, GRK2 induces SMO activation both by phosphorylating it and by increasing PI(4)P concentration (Jiang et al. 2016).

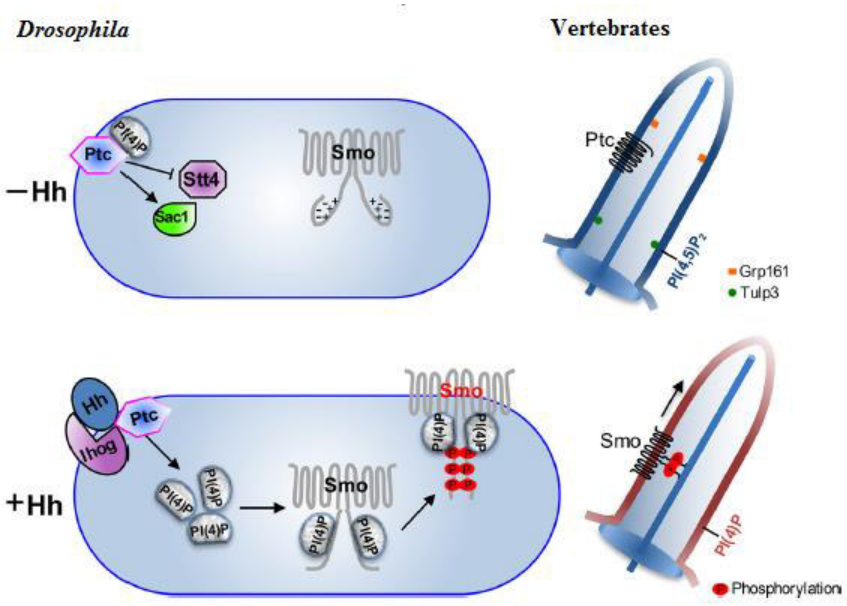

Figure 8: PI(4)P regulates Smo phosphorylation and membrane (left)/ciliary (right) accumulation.

In the absence of HH, STT4 low and SAC1 high activities lead to low levels of PI(4)P interacting with PTC. In vertebrates (right), the localization of Ptc1/2 and Grp161 to the primary cilium represses HH signal transduction. PI(4,5)P2 accumulates to the cilium. In the presence of HH, there is an increase in PI(4)P production as well as PI(4)P dissociation from PTC, which permits PI(4)P to bind to Smo. This binding leads to Smo activation by inducing Smo phosphorylation, dimerization and accumulation at the cilium. High levels of PI(4)P inhibit Ptc1/2 ciliary accumulation (Jiang et al. 2016).

PI(4)P also interacts with the arginine motif of the mouse SMO C-tail in a smilar manner. This points to a likely conserved role of the phospholipid between fly and mouse. Human PTC also interacts with PI(4)P and HH stimulation reduces this interaction, leaving more PI(4)P available to bind to and promote activity of SMO (Fig. 8) (Jiang et al. 2016).

Oxysterols, which are by-products of cholesterol oxidation, also have been shown to activate the HH pathway by directly binding to SMO. However, instead of binding to the C-tail, oxysterols bind to the N-terminal CRD of SMO. The activation of the HH pathway promoted by oxysterols, led to osteo-inductive effects *in vitro* and bone formation *in vivo*. As a result, oxysterols could be potentially used for the treatment of osteodegenerative disorder, e.g. osteoporosis (Jiang & Jia 2015).

6. Recruitment and activation of intracellular signalling multiprotein complexes by activated SMO

Activated SMO C-tail recruits the kinesin-like protein Costal2 (COS2) and the Ser/Thr kinase FU to the plasma membrane in order to allow HH signal transduction (Robbins et al. 1997; Jia et al. 2003; Lum et al. 2003; Ruel et al. 2003). The relationship between SMO, FU and COS2 is a very complex one. Mostly because these proteins interact on each other to influence high level of HH signalling activity. COS2, for instance plays both a positive and a negative role in the pathway. In absence of HH, COS2 contribute to the formation of CI repressor form, as well as its silencing. However, in presence of HH, COS2 is required for CI activation, which is able to go to the nucleus and promotes expression of target genes (Farzan et al. 2008), (Ding et al. 2013; Jia et al. 2003; Lum et al. 2003). The positive role of COS2 depends on its binding to FU, but not on FU phosphorylation of COS2 at Ser572 and Ser931 (Ranieri et al. 2012), (Liu et al. 2007), (Zadorozny et al. 2015). The evidence argues that COS2 functions as a scaffold protein for the FU molecules facilitating FU cross-phosphorylation and activation (Zadorozny et al. 2015). Interaction with FU also leads to COS2 translocation to the plasma membrane, where it interacts with SMO C-tail through two separate domains: one close to the 7 TM and the other in the C-terminus, forming a complex with the transducer (Ranieri et al. 2012), (Jia et al. 2003), (Lum et al. 2003).

Previous studies in my lab have shown that SMO and FU co-localise and that HH induces the SMO–dependent recruitment of FU to the plasma membrane. FU, in turn, plays an important role in the regulation of the subcellular localisation, stabilisation and phosphorylation of SMO. SMO phosphorylation by PKA/CK1 promotes phosphorylation of SMO by FU. The latter phosphorylation contributes to stabilise SMO at the plasma membrane and to high activity. Ultimately, this leads to high-throughput HH signalling. The boost in SMO activity in turn promotes an increase in FU activation (Fig. 9), which is required for its role in phosphorylating Cos2 and SU(FU) in order to promote CI full-length activation (Sanial et al. 2017). In summary, the two proteins establish a positive feedback that enhances signalling and resistance to PTC (Claret et al. 2007), (Sanial et al. 2017).

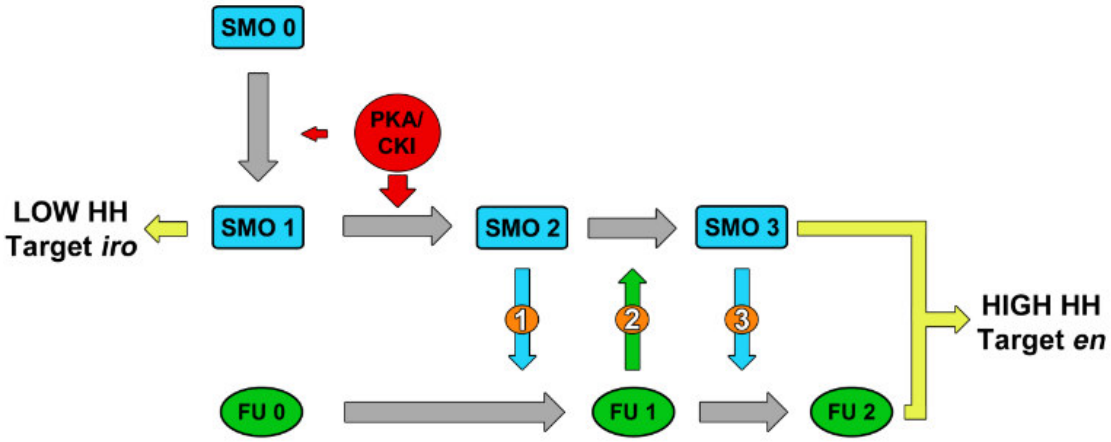

Figure 9: Model of how SMO/FU interact to promote high-throughput HH signalling.

The gradual phosphorylation of PKA and CK1 sites, due to the HH gradient, favours progressive SMO and, consequently, CI FL accumulation. The PKA/CK1 phosphorylation of SMO (SMO 1), induced by low levels of HH, blocks enough CI FL processing to allow expression of low target genes, e.g. iro and dpp. More HH promotes higher levels of SMO phosphorylation (SMO 2), which translates into higher activity. At this point, a positive feedback loop between both protein is generated in which SUMO2 induces Fu activation (FU1) (step 1), FU1 phosphorylates SMO C-tail (step 2), increasing even more SMO activity (SMO 3), and SMO 3 promotes further activation of FU (FU 2) (step 3) and action on its downstream targets (Sanial et al. 2017). *SMO/FU0, 1, 2 (and 3 for SMO) correspond to increasing levels of SMO or FU activation, respectively.*

However, despite all the knowledge gathered on this pathway and its key players, the mechanisms behind SMO activation and function are not altogether understood. A thorough knowledge of SMO regulation and activity may lead to the uncovering of new therapeutic approaches to combat pathologies caused by deregulation of the HH pathway.

For these reasons, the lab searched for novel partners of SMO.

.

E. The RNA-binding protein SMAUG

SMAUG is an RNA-binding protein that has been shown to regulate the fate of mRNAs during early development of the fly embryo either through an inhibition of their translation and/or by promoting their deadenylation (Paris et al. 2016). It thus plays a central role in the clearance of two-thirds of the unstable maternal mRNAs during the maternal-to-zygotic transcription transition embryogenesis (Chen et al. 2014), (Luo et al. 2016). It also controls the establishment of the fly embryo's antero-posterior polarity by repressing the translation of a key determinant of the posterior identity, *nanos* (Dahanukar et al. 1999; Smibert et al. 1996). It also regulates *nanos* mRNA translation in larval neurons. In all these studied cases, SMAUG acts as a platform that brings together target mRNAs (bound via its SAM domain), and proteins that repress them, such as, the initiation factor competitor eIF4G or Argonaute 1 which prevent translation or cytoplasmic deadenylases, such as CCR4-NOT (Fig. 10).

In mammals, two *smaug* genes are present, with SMAUG1 being mostly expressed in the nervous system, where it controls synapsis morphogenesis and function, through the control of specific mRNAs (Fernández-Alvarez et al. 2016) (Zheng et al. 2010). Strikingly, synaptic activity can lead to the transient solubilisation of the SB, allowing the release of stored mRNA (Zhao et al. 2007).

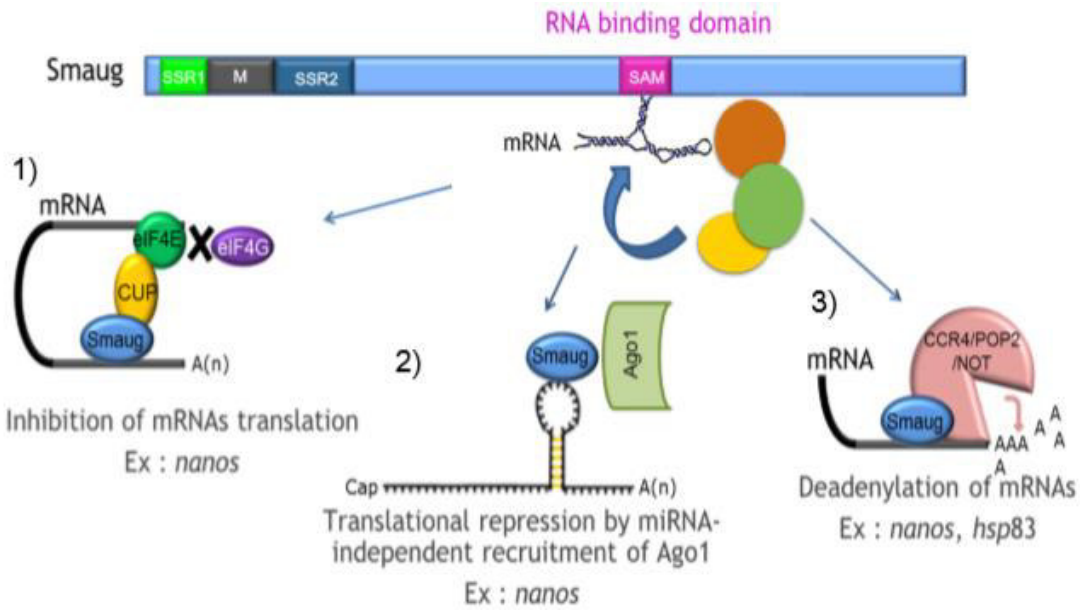

Figure 10: Action mechanisms of SMAUG.

SSR1 (green box): SMAUG Similarity Region 1; M: Middle region (grey box); SSR2: SMAUG Similarity Region 2 (blue); SAM: Steril Alpha Motif (fuchsia). 1) SMAUG repressed expression of nanos mRNA by binding to CUP and the translation initiation factor competitor eIF4E, preventing in this way the recruitment of the initiation factor eIF4G to the mRNP (mRNA-protein complexes) (Nelson et al. 2004). 2) The binding of SMAUG to nanos mRNA recruits Argonaute 1 (Ago1), which leads to nanos translational repression in a miRNA-dependent manner (Paris et al. 2016). 3) SMAUG is able to recruit major cytoplasmic deadenylase complexes, such as CCR4-NOT, which leads to mRNA poly(A) shortening and, consequently, degradation (Paris et al. 2016).

Two postgraduate students from my lab, C. Argüelles and L. Bruzzone have confirmed this interaction between SMO and SMAUG by biochemical studies, and shown that they could co-localize in cultured cells. Moreover their results indicate that SMAUG could play a role as a novel member of the HH pathway since:

(i) SMAUG is expressed, albeit at low levels in the wing imaginal disc, where it partially localizes with SMO.

(ii) SMAUG overexpression upregulates HH signaling activity and SMO levels. Notably, these effects require its RNA binding domain (SAM domain), suggesting that SMAUG acts on HH signaling via its association to one (or several) mRNA(s).

Finally, their recent data based on the co-expression of SMO and SMAUG in cultured cells, indicates that HH could control the subcellular localization of SMAUG, its interaction with SMO and its phosphorylation.

Altogether by highlighting an unexpected relationship between HH/SMO signaling and SMAUG, these data indicate that mRNA regulation might finely tune the levels of HH signaling and provide novel evidence for regulation of SMAUG.

F. Main aims of my project

My project was focus on the relationship between SMO and SMAUG. By employing complementary, cellular, biochemical and genetic methods, my specific aims were:

(i) Better analyse the co-localisation between SMO and SMAUG

(ii) Characterize a phosphorylation of SMO that appears to control SMO/SMAUG interaction, and identify the kinase responsible for this phosphorylation

(iii) Better characterize the role of SMAUG in HH signalling;

VII. Materials and methods

A. Drosophila experiments

1. Fly stocks and Crosses

Fly lines used are*: w1118*, *fu¹ MS1096/FM7*, *UAS-smaug-RNAi (M1M)* and *UAS smaug-RNAi (M2M)* (BestGene Inc) (Table 1). The two *UAS-smaug-RNAi* were built just before my arrival. The system used to generate these two last lines was the *PhiC31* integration system, leading to the insertion of a *UAS-smaug-RNAi* transgene into the fly genome, in the same locus of chromosome 3. Two lines were obtained corresponding to different site-specific recombination events, of the same transgene, at the same locus. They were called **M1M** and **M2M**.

All fly stocks were transferred monthly to fresh tubes.

Genotype	Features	Source
w1118	Chromosome **I** harbours the ***white* mutation** that confers white eyes in homozygosity and hemizygosity.	A. Plessis
fu1MS1096/FM7 *('/' separates homologous chromosomes)*	Chromosome **I** harbours a mutation in one of ***fused* alleles** that causes wing patterning defects (fusion of the proximal region of LV3 and 4) in homozygosity and hemizygosity. ***MS1096*** is a *Gal4* driver. **FM7** is the balancer chromosome (see text).	A. Plessis
UAS-smaug-RNAi(M1M) and ***(M2M)***	Chromosome **III** integrates a sequence of 21 nucleotides that targets a region of SMAUG between the two SSRs, in order to downregulate SMAUG expression.	BestGene Inc

Table 1: Fly lines.

The *fu gene* is carried by the X (first) chromosome. *fu¹* is a well-studied allele of *fu* that is known to affect its kinase activity (Alves et al. 1998). *fu¹* is a null allele that was recently obtained in the lab by the CRISPR method. **FM7** (1st multiply-inverted 7) is a balancer of the X chromosome (chromosome I). Balancer chromosomes carry multiple inversions that prevent

recombination events (crossing-over) with the homologous chromosome. Balancers chromosome carry lethal or sterile mutations (to avoid the loss of the non-balanced chromosome) and a dominant marker mutation that allows the operator to follow them in mating schemes. This characteristics are quite advantageous, for instance the FM7 in the *fu*^{a}*, MS1096* line carries the marker dominant *Bar* (*B*) mutation, which confers kidney-shaped eyes in heterozygosity and slit-shaped eyes in homozygosity and hemizygosity. This marker mutation allowed to select heterozygous female flies for the crosses. This was useful because females homozygous for the *fu*^{a} mutation are sterile.

Smaug^{0} is on the third chromosome and *smaug*^{0} homozygous mutant females *are* sterile. We therefore balanced the *smaug*^{0} mutation that we obtained during my stay in the lab by the CRISPR method with the TM3 or TM6 balancers.

The *smaug-RNAi* transgene was expressed in the wing disc thanks to the UAS/Gla4 system (Fig. 11). We used the Gal4 driver, *MS1096* which is expressed at high levels throughout the wing imaginal disc, with a higher expression in the cells of the dorsal compartment (Wang et al. 1999).

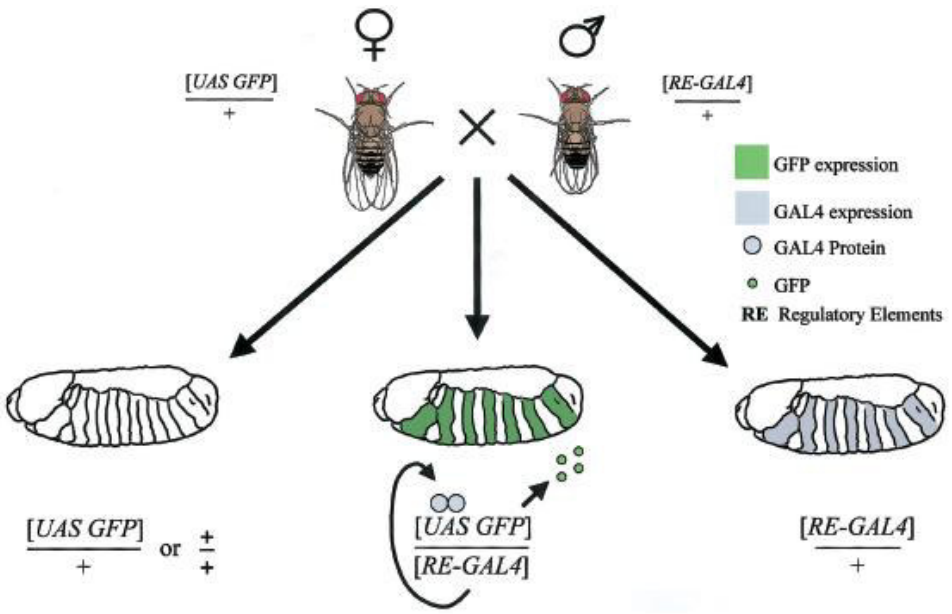

Figure 11: The Gal4/UAS system.

Parental generation (upper line): a female fly (left) that has a GFP gene under the control of the cis-regulatory element Upstream Activating Sequence (UAS) is mated to a male fly (right) that expresses a Gal4 gene under the control of endogenous regulatory elements. A fly from the resultant progeny, carrying both parts of the system (middle fly, lower line) is produced, and the

trans-element GAL4 binds to the UAS and drives expression of the GFP gene in an alternating segmental pattern. Horizontal line separates homologous chromosomes. '+' represents wildtype chromosome (Duffy 2002).

The following crosses were carried out:

1. *fu¹,MS1096/FM7* X *UAS-smaug-RNAi (M1M)/+*
2. *fu¹, MS1096/FM7* X *UAS-smaug-RNAi (M1M)/+*
3. *fu¹,MS1096/FM7* X *w1118/Y* (control cross)

The crosses were kept at 25°C, and transferred to new tubes daily.

Crosses nomenclature: '/' separates homologous chromosomes; "," the genes or transgenes present on the same chromosome; '+' corresponds to wildtype chromosomes.

2. Wing imaginal disc immunostaining

Wandering third instar larvae were collected, rinsed in PBS1x and selected according to two selection criteria (males were selected under appropriate fluorescent stereo-microscope) to ensure that we had *fu¹, MS1096/Y* males. The larvae were cut around two thirds from their heads and inverted inside out, to expose the wing discs and facilitate their staining. The larvae half containing the head was kept. The inverted carcasses were placed in PBS1x in a 1.5 mL microcentrifuge tubes on ice (no longer than 15 min). Subsequently, the PBS1x was removed and replaced by 1 mL 4% Paraformaldehyde (PFA). All steps concerning the handling of PFA, were carried out under the hood. The tubes were then placed on a nutator for 20 minutes. It was important not to leave the carcasses in the fixative agent for more than 20 min, as it weakens the tissues. After fixation, the PFA was promptly removed, and the larvae carcasses quickly rinsed twice with PBS1x Triton 0.3% solution (PBT) and the washed thrice, 10 minutes/wash, with PBT. Subsequently, the tissues were "blocked" (to reduce the background) with 1 mL BBT (PBS1x, triton 0.3%, BSA 0.1%, NaCl 25 mM) for 30 min on a nutator. After, the BBT was removed, and the tissues incubated with the primary antibody cocktail in a 50 mL-BBT solution overnight at 4°.

The following day, the antibody solution was removed, and the tissues were rinsed once and washed thrice with PBT for 10 min/wash on a nutator. The secondary fluorescent antibody was

added in 100 µL of BBT, and the tissues were incubated for 2 hours on a nutator at room temperature (RT). During this step and on, the tubes were enveloped in aluminium foil to avoid bleaching of the antibody fluorescence. This was followed by four washes with PBT (10 min each) on a nutator. The second wash was with PBT Hoesht (1/400) in order to mark nuclei. The tissues were then incubated with a drop of mounting medium (CITI FLUOR AF1) overnight at 4° before mounting and imaging

Wing imaginal disc images were acquired with a Leica SP5 confocal microscope, analysed with ImageJ (National Institute of Health), and assembled with Photoshop (Adobe, San Jose, CA).

Primary antibodies: 1:1000 Mouse anti-Ptc (DSHB), 1:25 Mouse anti-Col (M. Crozatier), 1:5 Rat anti-Ci (Gift from Robert Holmgrin), 1:1000 mouse anti-SMO (DHSB, clone 20C6) and 1:100 Rabbit polyclonal anti-Gal4 (Santa Cruz Biotechnology). Secondary antibodies: Alexa Fluor 488 Goat anti-Rabbit (Invitrogen), Alexa Fluor 555 Goat anti-Mouse (Invitrogen) and Alexa Fluor Goat anti-Rat (Invitrogen). The secondary antibodies were used at a dilution of 1:100.

3. Fly wing

The flies, conserved in 1.5 mL micro-centrifuge tube containing ethanol 70%, were placed in a petri dish filled with ethanol 70%. The right wings were removed, rinsed in water, and mounted in Hoyer's medium.

Wing images were acquired at a 150x magnification using the Keyence VHX-2000 Digital Microscope, and assembled with Photoshop (Adobe, San Jose, CA).

4. Statistics

The *p-Values* concerning the wing experiments were calculates using an online Fisher's test at https://marne.u707.jussieu.fr/biostatgv/?module=tests/fisher, May 18th, 2017).

B. Cloning procedures

Cloning strategies were developed using *Serial Cloner 2.6*

1. By restriction enzyme-ligation procedures

a) Enzymatic Digestion

Plasmid DNA or PCR products were digested using FastDigest® restriction enzymes (Thermofisher, following manufacturer's instructions) exploiting restriction sites present in the plasmid vectors or incorporated in the PCR fragments. The vectors were digested in the same way as their intended inserts.

b) DNA sequence purification

The DNA fragments from each digestion reaction were resolved in agarose gel (percentage of agarose was according to the size of fragment of interest, ranging from, 0.7 to 1% in TBE buffer). They were excised from the gel and purified (NucleoSpin® Gel and PCR and PCR Clean-up), in order to avoid contamination by the digested fragments besides the one of interest or by partially digested vectors. .

c) Ligation

It was done withT4 DNA ligase (Thermoscientific) following manufacturer's instructions.

2. By the Gateway technology.

Gateway Technology (Invitrogen, following the manufacturer's instructions) was employed to mediate recombination of mutant transgenes from pENTR clones (Entry vectors) to pAct5C-GW-TAG (Destination vectors). The latter vectors allowed expression of the tagged proteins under the constitutive promoter 5Act5C in cultured cells. The principal of the Gateway Technology is outlines in Fig. 12.

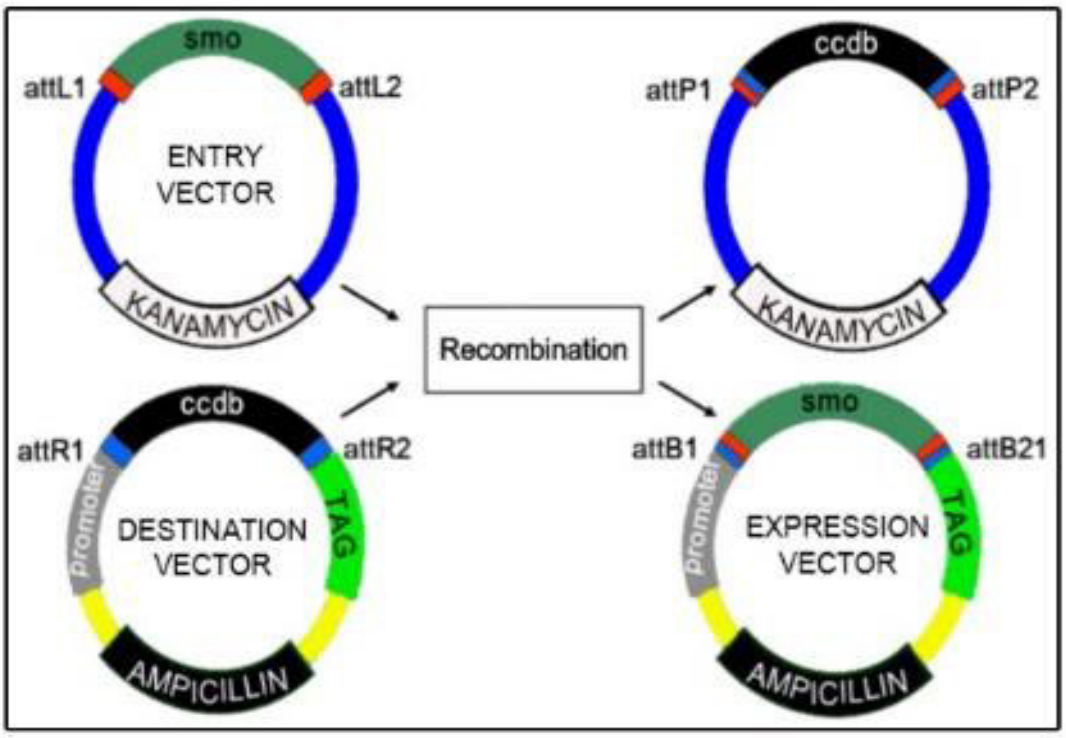

Figure 12: Gateway site-specific recombination system.

Gateway Cloning Technique allows transfer of DNA fragments between different cloning vectors while maintaining the reading frame. The system requires the initial insertion of a DNA fragment into a plasmid with two flanking recombination sequences "att L 1" and "att L 2", to develop a Gateway Entry clone. The gene cassette in the Gateway Entry clone can be transferred into any Gateway Destination vector (Invitrogen nomenclature for any Gateway plasmid that contains Gateway "att R" recombination sequences and elements such as promoters and epitope tags, but not ORFs) using the proprietary enzyme mix, "LR Clonase". The result is an "Expression vector" containing att B sites, flanking gene of interest, ready for gene expression. This construct is selected on Ampicillin, in the Top10 E. coli strain in which the ccbd gene has a toxic effect in this line.

3. Chemo-transformation:

1 ng of plasmid DNA was mixed with 50 µl of "One Shot TOP10" chemo-competent *E. coli* and incubated on ice for 15 min. Thereafter, bacteria were transformed by heat-chock, exactly 30 sec at 42°C, and placed on ice for 2 min more. 200 µl of LB medium were added and bacteria were incubated 45 min at 37°C in order to express resistance to the selection antibiotic.

The bacteria were then plated on an agar plate containing the appropriate selection antibiotic for the plasmid, and incubated at 37°C overnight.

4. Clones selection and validation

a) PCR on colony:

Bacterial cells from individual colonies were lysed in water (5 min at 95°C), and added directly to the PCR reaction. The initial heating step causes release of the plasmid from the cell, which can then be used as template for the amplification reaction. A primer specific for the insert and a primer specific for the vector were used to confirm the presence and correct orientation of the insert. Taq DNA polymerase (Thermoscientific) was used according to manufacturer's instructions.

b) Restriction enzyme digestion:

Plasmid DNA was isolated from different bacterial colonies using DNA preparation by alkaline lysis (described below). After which, appropriate FastDigest® restriction enzymes (Thermofisher, following manufacturer's instructions) were chosen, one to cut the backbone vector and one to cut the insert. Linear DNA was resolved by size on agarose gel, to characterize insertion.

c) DNA preparation by alkaline lysis:

I inoculated bacteria in 4 mL of LB medium with antibiotic (1000x ampicillin). On the following day, I centrifuged 2 mL of culture for 5min at 11000 rcf at room temperature. The supernatant was discarded, and cell pellet re-suspended in 200 µl of re-suspension buffer (50 mM Glucose, 25 mM Tris pH8, 10 mM EDTA pH8). After complete re-suspension, 400 µl of lysis buffer (0.2 M NaOH, 1% SDS) was added, and the solution gently mixed and incubated for 5 min at RT. Thereafter, I added 300 µl of neutralization buffer (3M potassium, 5M acetate) to the solution and mixed it thoroughly. I then centrifuged the mixture twice: 5 min at 11000 rcf at RT, I recovered the supernatant to a new tube each time. After the second centrifugation, I added 1 mL of 2-Propano 100% (Analar Normapur®) to the supernatant, and mixed by inverting the tube. After another centrifugation of 10 min at maximum speed (RT), I added 500 µl of 70% Ethanol. The solution was subjected to a final 10 min centrifugation at maximum speed. The supernatant

was discarded, the pellets vacuum-dried for 5-10 min, and finally re-suspended in 50 µl of water with RNAse A.

d) Sequencing

DNA of selected clones was prepared with NucleoSpin® Plasmid Mini kit, and sent for sequencing at Eurofins Genomics. Sequence was confirmed by Sanger sequencing. We used BLAST (*NCBI*) software: to compared the sequencing results to reference sequences.

e) DNA preparation:

After confirmation of correct sequence, Pure Yield™ MIDI prep system was used to prepare plasmid DNA for storage and cell transfection.

C. SMO constructs

Some of the *smo* mutant constructs that I employed in my experiments were built in *pENTR* vectors by the laboratory before my arrival. I used Gateway recombination technology, detailed in Fig. 12, to re-clone these constructs into *p5Act5C-GW-HA*. This vectors constrains the promotor of the Actin 5C drosophila gene and a sequence encoding three copies of the HA epitope. A gateway rebombination sites was present before the HA Tag, in order to insert the gene of interest in phase with it. I also used this technology to clone *pENTR-smo*, $smo^{\Delta 1004}$ and *smoΔ958* into *p5Act5C-GW-mCherry*, and *pENTR-smaug* into *p5Act5C-Gfp-GW* that respectively allow a mCherry fusion to the C-terminal part of SMO and a GFP to the N-terminal end of SMAUG.

After recombination, I performed chemo-transformation, followed by clone selection using either PCR on colony or restriction digestion.

Some *smo* constructs, such as the one encoding SMO c14A (see bellow), were generously provided by researchers (Table 1) in *pRmHA3-smoc14-Gfp* into a *pAct-smo-HA* vector by enzymatic digestion of both vectors with EcoRI and SexA1, followed by DNA purification of a fragment of 735 bp and a fragment of 8050 bp from gel (sizes predicted by *Serial Cloner 2.6*). Then, ligation, chemo-transformation, plasmid preparation and sequencing followed.

.

smo mutant	Plasmid	Tag	Features	Origin
680-3 SA	***pUASTattb***	**(N-terminus) Myc**	⟶ A of residues 680 and 683	**Jiang *et al.* 2014**
680 SD	*idem*	*idem*	⟶ D at 680 and 683 residues	*idem*
SD 680-3 SA	*idem*	*idem*	PKA/CK1 ⟶ D; 680 and 683 ⟶ A	*idem*
SD 680-3 SD	*idem*	*idem*	PKA/CK1 ⟶ D 680 and 683 ⟶ D	*idem*
CKII SA	*idem*	*idem*	816-19, 843 ⟶ A	**Jia *et al.* 2010**
CKII SD	*idem*	*idem*	816-19, 843 ⟶ D	*idem*
CL-II SA	*idem*	*idem*	626-7, 633-4 ⟶ A	**Li *et al.* 2016**
CL-II SD	*idem*	*idem*	626-7, 633-4 ⟶ D	*idem*
SD CL-II SA	*idem*	*idem*	PKA/CK1 ⟶ D; 626-7, 633-4 ⟶ A	*idem*
SD CL-II SD	*idem*	*idem*	PKA/CK1 ⟶ D; 626-7, 633-4 ⟶ D	*idem*
S972 A	***p5Act5C***	***HA (C-terminus)***	972 ⟶ A	**Built in the lab**
S989 A T993 A	*idem*	*idem*	989, 993 ⟶ A	*Idem*
T1003 A	*idem*	*idem*	1003 ⟶ A	*Idem*
5S/T A	*idem*	*idem*	972, 989, 993, 1003, 1020 ⟶ A	*Idem*
PKA-SD	*idem*	*idem*	667, 687, 641 ⟶ A	*Idem*
SD c14 A	***pRmHa3***	***GFP (C-terminus)***	PKA/CK1 ⟶D; 604, 606, 610, 612, 626-7, 629,633-5, 651, 655, 658-660, 675, 680, 683 ⟶ A	**Maier *et al.* 2014**
SD c12 SD	*idem*	*idem*	PKA/CK1 ⟶ D; 604, 606, 610, 612, 626-7, 629,633-5 ⟶ A	*idem*
SD	*idem*	*idem*	PKA/CK1 ⟶ D	*idem*
c14 A	*idem*	*idem*	604, 606, 610, 612, 626-7, 629,633-5, 651, 655, 658-660, 675, 680, 683 ⟶ A	*idem*

Table 2: smo mutant constructs used to transfect Cl8 cells for Western Blotting or Co-IP experiments.

Ser and Thr of smo C-terminal tail coding sequence have been mutated to either Alanine (⟶ A) or Aspartic acid (⟶ D). All plasmids contain a marker gene.

Other constructs	Plasmid	Tag	Origin
hh n-terminal	***p5Act5C***	*no tag*	**Built in the lab**
gal4	*idem*	*no tag*	*idem*
smaug	*idem*	**Myc**	*idem*

Table 3: Other constructs used to transfect Cl8 cells for Western Blotting or Co-IP experiments.

All plasmids contain a marker gene of resistance to ampicillin.

Cell imaging constructs	Plasmid	Tag	Origin
smo	*p5Act5C*	*mCherry (C-terminus)*	**Built in the lab**
smo Δ 1004	*idem*	*idem*	*idem*
smo Δ 958	*idem*	*idem*	*idem*
smaug	*idem*	GFP (N-terminus)	*idem*

Table 4: Plasmid constructs used to transfect Cl8 cells for fluorescent cell imaging studies.

All plasmids contain a marker gene of resistance to ampicillin.

D. RNA interference (RNAi)

VALIUM20 (TRiP) vectors were used for shRNA-mediated knockdown of expression of **CK1α, Gilsh, CKIIβ, aPKC, PKAc1, Gprk2 and GFP** in Cl8 cells. In the lab, shRNAs (21 bp) were cloned into **VALIUM20** vectors following the protocol for "Cloning hairpins into Valium or Walium vectors" prepared by Jian-Quan Ni, Matt Booker and Nobert Perrimon (Yang-zhou et al. 2012). This protocol can be found online at https://fgr.hms.harvard.edu/cloning-and-sequencing (May 20th, 2017).

In VALIUM20 vectors, the expression of the shRNA is under the control of the UAS, in other words. As the vectors do not contain *Gal4* gene, I had to provide to the cells through transfection (Table 4).

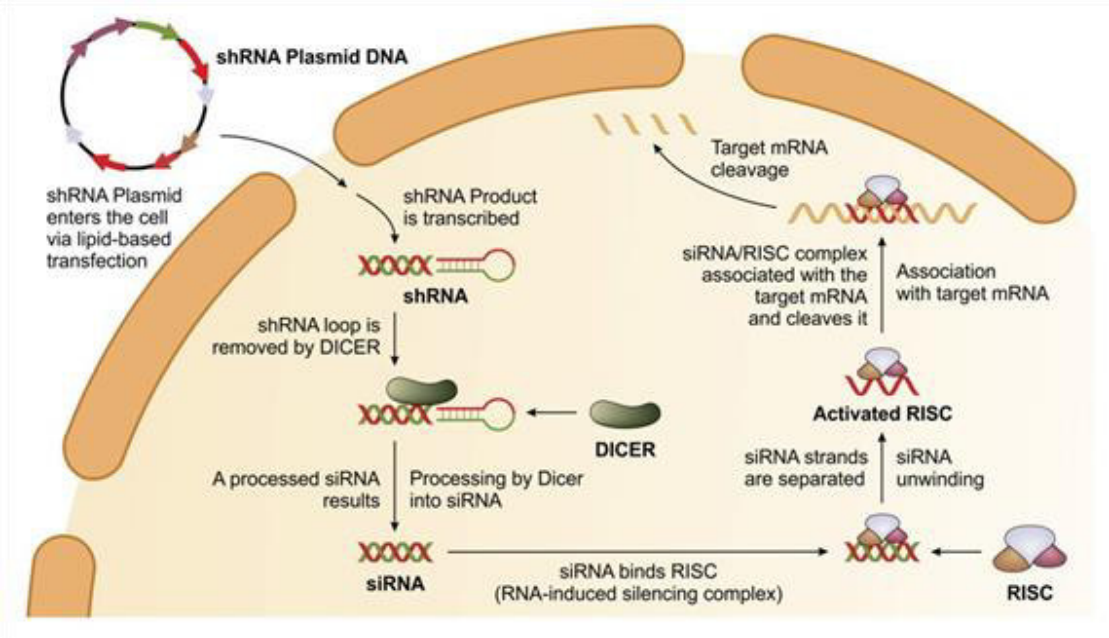

Figure 13: Mechanism of action of shRNA-plasmid gene silencer.

shRNA is processed by Dicer to form siRNA. The latter binds to the RISC complex; siRNA sense strain is degraded and the antisense (guide) strain remains at which point the whole complex is activated.

E. Cell culture and Transfection

Clone 8 (Cl8) cells are derived from the drosophila's wing imaginal disc, and are responsive to HH (Chen et al. 1999).

Cl8 cells were cultured in complete medium: Shields and Sang M3 Insect Medium with (Sigma S35652) with 2% de-complemented Bovine Serum, 2.5% fly extract, 0.0125 IU/mL Human Insulin (Sigma 19278) and 1x Penicillin-Streptomycin (Sigma 4458), and incubated at 22°C without CO2. The cell culture was split every 4/5 days after re-suspension with scraper, and the splitting dilution was 1/6, 4 mL/25 cm^2 flask. For transfection of Cl8 cells, TransIT ® - Insect (Mirus) was used following manufacturer's instructions.

Cells were transfected approximately 24 hours after being plated in complete medium at a density of 1.6-3.2 x 105 cells/mL and grown overnight. The conditions for optimal transfection are described in Table 2.

Culture vessel	24-well plate	12-well plate
Surface area	1.9 cm^2	3.8 cm^2
Complete growth medium	0,4 ml	0,8 ml
Serum-free medium	50 µl	100 µl
DNA (1 µg/µl stock)	0.5 µl	1 µl
*Trans*IT-Insect Reagent	2µL	4µL

Table 1: Optimised conditions for Cl8 cells transfection

F. Cell extraction, Western Blotting and immunostaining

72 hours post-transfection, cells were re-suspended, centrifuged (850 rcf, 5 min, at RT), washed with PBS1x, and centrifuged again. Subsequently, the cells were incubated with lysis buffer: 1% NP40, 150 mM NaCl, 50 mM Tris HCl pH 8.0, 0.5% Na Deoxycolate and 10% Glicerol with Complete, EDTA-free Protease Inhibitor cocktail (Roche) and Phosphatase Inhibitor Cocktail (Roche), during 15 min on ice. Note: from this point onward, cell samples were kept on ice. The lysate was then centrifuged (12000 rcf, for 10 min at 4°). Protein quantification was determined by Bradford's method with BradfordUltra Detergent (Expedeon) following the manufacturer's instructions. 30 µl of each protein sample were mixed with 1x loading buffer: Laemmli sample buffer (Biorad) and 0.1 M DTT.

The protein samples were resolved by Anderson gel (10%) (Table 3) in a mini-protean apparatus (Bio-Rad): 90 min at 150 V (constant voltage). Following migration, the proteins were transferred onto Nitrocellulose membrane (0.2 µM, Amersham Protran) in the same apparatus for 75 min at 100 V. After transfer, the membrane was incubated for 45 min in a solution of 0.1 % PBS Tween and 5 % fat milk in powder (blocking solution) at RT to avoid non-specific binding of the antibodies. The membrane was then incubated with the primary antibody (diluted in blocking solution) with gentle rotation at 4° overnight. The following day, the membrane was washed 5 times (5 min/wash) with PBS Tween, and incubated with the secondary antibody (diluted in blocking solution) with gentle rotation for 2 hours at RT. Then the membrane was washed again 5 times with PBS Tween. Immune-labelled bands were revealed using the enhanced chemiluminescence (ECL Select, Amersham) protocol on LAS-3000 imager (Fujifilm).

Primary antibodies: 1:1000 Rat monoclonal anti-HA (Roche Diagnostics); 1:2000 Rabbit anti-GMAP (Sigma, gift from Laurent Ruel); 1:1000 Mouse monoclonal anti-Myc (Millipore). Secondary antibodies conjugated with HRP: anti-Rat (JacksonImmuno); anti-Mouse (Sigma). The secondary antibodies were used at 1:10000 dilution.

Antibody Stripping solution x1 (Gene Bio-Application L.T.D) was used for the reblots.

	Resolving gel	Stacking gel
Ratio Acrylamide/Bis-acrylamide	77	37.5
Final volume (mL)	5	2.5
Gel %	10	5
40 % Acrylamide	1.25 mL	0.3125 mL
2 % Bis-Acrylamide	0.32 mL	0.17 mL
1 % Tris pH 8.8	1.875 mL	0.3125 mL
10 % APS	50 µl	25 µl
100 % TEMED	4 µl	4 µl
Water	1.50 mL	1.50 mL

Table 2: 10 % Anderson gel recipes.

In Anderson Gel, the ration between acrylamide and bis-acrylamide changes according to the gel percentage. It allows a more accurate separation of the proteins, and, consequently, to distinguish different protein phosphorylated forms. The principal of principal of protein separation is the same as that of the classic SDS-Page.

G. Immunoprecipitation for Co-IP assay using magnetic separation

Following protein extraction and quantification as above, lysis buffer (plus anti-phosphatase and anti-protease) was added, up to a volume of 500 µl, to 1 mg of extracted protein/sample. From these samples, 25 µl of each extract were taken and mixed with loading buffer and 0.1 M DTT, frozen in liquid nitrogen, and stored at - 80° overnight. They correspond to the "*Input (Inp)*" fraction. 2 µg of antibody against the protein tag were added to the remaining 475 µl of each sample, and incubated with gentle rocking at 4° overnight. The following day, extract-antibody mixes were incubated with pre-washed A/G Magnetic Beads (Thermo Scientific) on a rotating

wheel for 2 hours at 4°. The tubes were placed in a magnetic rack to recover the beads. 25 µl of supernatant of each tube were taken and mixed with loading buffer and 0.1 M DTT. They correspond to the "*Supernatant (Sup)*" fraction. The beads were washed thrice with lysis buffer, 5 min/wash on a rotating wheel at 4°. The bead pellets were re-suspended in 25 µl loading buffer, 5 µl DTT 1M and 20 µl lysis buffer, before being heated for 3 min at 95°. These fractions, minus the beads correspond to the "*Immunoprecipitated (IP)*" Half of each IP sample (minus beads), the Input and Supernatant were loaded on a 10% Anderson Gel, as described above.

IP antibodies used: Rabbit anti-c-Myc (BETHYL); Mouse monoclonal anti-Myc (Millipore).

H. Cell fixation for fluorescent cell imaging

48 hours post-transfection (Table 4), Cl8 cells were re-suspended and pipetted onto a coverslip coated with 2 µl of concanavalin A (1 mg/mL). They were incubated for 25 min, at room temperature, in order to allow the cells to adhere to the concanavalin in the coverslip. Subsequently, the supernatant was aspirated, and the cells washed with PBS1x for 5 min. The cells were then incubated with 4% PFA for 20 min. The fixative agent was removed, and the cells were rapidly washed with PBS1x, followed by three additional washes, 5 min each. Note: the second wash was with PBS1x Hoesht (1:1000). The cells were mounted with CITI FLUOR AF1.

Cell images were acquired with a 63x magnification oil objective lens (numerical aperture: 1.4) with a Leica SP5 confocal microscope, analysed with ImageJ (National Institute of Health), and assembled with Photoshop (Adobe, San Jose, CA).

VIII. Results

A. SMO and SMAUG co-localise in co-transfected Cl8 cells, with or without HH, in an interaction-dependent manner

Previous experiments in the lab have shown that SMO and SMAUG interact with each other, but do they also co-localise? And if they do, is interaction required? My first aim was to answer these questions.

For that purpose, I used Cl8 cells transfected with SMO and SMAUG that were fused to fluorescent proteins.These cells are derived from the wing imaginal disc and are widely used to study the Hh signaling (Chen et al. 1999).

1. Choice of the fluorescent tag

Preliminary data, obtained in the lab by fluorescent cell imaging, indicated that SMO-RFP and GFP-SMAUG co-localise in presence and absence of HH. However, SMO-RFP signal was very weak, probably due to the RFP tag. To solve this problem, I replaced the RFP by another red fluorescent protein, mCherry, which presented a higher photo-stability and resistance to photo-bleaching.

I first compared, two different tag combinations: GFP-SMAUG/SMO-mCherry and mCherry-SMAUG/SMO-GFP (data not shown). The GFP-SMAUG and SMO- mCherry, gave a good signal to background ratio. The mCherry-SMAUG was however difficult to detect, but SMO-mCherry gave a satisfactory signal. This is why I decided to used GFP-SMAUG/SMO-mCherry for my subsequent experiments.

2. SMO and SMAUG co-localise in Cl8 cells with and without HH

Then, I compared the subcellular distribution of SMO-mCherry and GFP-SMAUG alone or together. In order to examine the effect of HH on SMO-mCherry and GFP-SMAUG localisation and potential co-localisation, I did in parallel a set of experiments without HH, and another with HH.

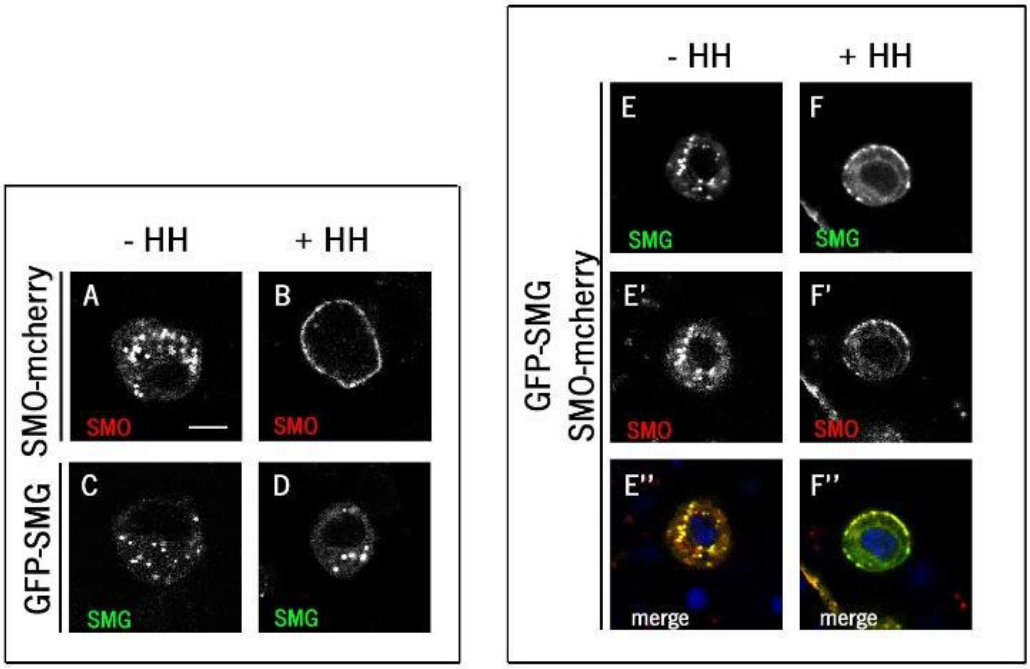

Figure 14: Subcellular distribution of SMO-mCherry and GFP-SMAUG in presence or absence of HH.

Fluorescent images of transfected Cl8 cells expressing SMO fused to mCherry (at its C-terminus, SMO-mCherry*) (A, B, E' and F') and SMAUG fused to GFP (at its N-terminus,* GFP-SMG*) (C, D, E and F) alone (A-D) or together (E-F), with ('+') or without ('-') HH, as indicated. Note that fusions of tags have been shown not to affect SMO and SMAUG respective activities. Merge images are shown in E'' and F''. Scale bar represents 10 µm and is the same for all cells images in Fig. 14 and 15. Here and in Fig. 15, images were acquired at 63x magnification, with a Leica SP5 confocal microscope.*

As expected, SMO-mCherry was found in cytoplasmic vesicles in absence of HH (Fig. 14 A) and it was mainly localised at the plasma membrane in presence of HH, (Fig. 14 B). In absence of HH, GFP-SMAUG was found in foci in the cytoplasm (Fig. 14 C) and no obvious change could be observed in response to HH (Fig. 14 D).When GFP-SMAUG and SMO-mCherry were co-expressed in absence of HH, they co-localised in foci in the cytoplasm (Fig. 14 E-E''). It appears that all foci that are SMO-mCherry plus, are GFP-SMAUG plus, and vice-versa. In response to HH, GFP-SMAUG changed localisation and now co-localised at the plasma membrane with SMO-mCherry (Fig. 14 F-F'').

In summary, GFP-SMAUG and SMO-mCherry co-localise in presence and absence of HH, and GFP-SMAUG is found at the plasma membrane in presence of HH only if SMO-mCherry is co-expressed.

3. SMO and SMAUG interaction is required for their co-localisation

The interpretation of the co-localisation of two proteins is limited by the optical resolution. This is why I could not infer whether the SMO and SMAUG proteins co-localised because they were in the same complex (or attached to the same structure), or because they interacted together. The recruitment of GFP-SMAUG at the plasma membrane in presence of HH that occurred only in the presence of SMO-mCherry, suggested however that it was due to their interaction, but it did not prove it.

I, therefore, tested whether the interaction between SMO and SMAUG is required for their co-localisation. I took advantage of two deleted forms of SMO: SMOΔ958-mCherry and SMOΔ1004-mCherry which lack the region after the residue 958 or 1004, respectively. SMOΔ958-mCherry, which did not interact with GFP-SMAUG due to the deletion of the SBS, was used to answer my question andSMOΔ1004-mCherry, which interacted with GFP-SMAUG, was used as control.

Similar to what was observed with SMO-mCherry (Fig.14 A), SMOΔ1004-mCherry and SMOΔ958-mCherry were found in punctuate structures in absence of HH (Fig. 15 A, E) and at the plasma membrane in presence of HH (Fig. 15 B, F). This shows that the two deletions do not destabilise SMO nor hinder it from going to the plasma membrane in response to HH. In cells expressing SMOΔ1004-mCherry and GFP-SMAUG together, the proteins co-localised in the cytoplasm in absence of HH (Fig.15 C-C''). When HH was present, SMOΔ1004-mCherry and GFP-SMAUG still co-localised at the plasma membrane (Fig.15 D-D''). Thus, in the respect of co-localisation with GFP-SMAUG, SMOΔ1004-mCherry behaved just like SMO-mCherry. In contrast, SMOΔ958-mCherry and GFP-SMAUG did not co-localise in absence of HH. The GFP-SMAUG foci were clearly separated from those with SMOΔ958-mCherry (Fig. 15 G-G''). Moreover, in presence of HH, GFP-SMAUG remained in cytoplasmic foci, and did not co-localised with SMOΔ958-mCherry that was at the plasma membrane (Fig. 15 H-H'').

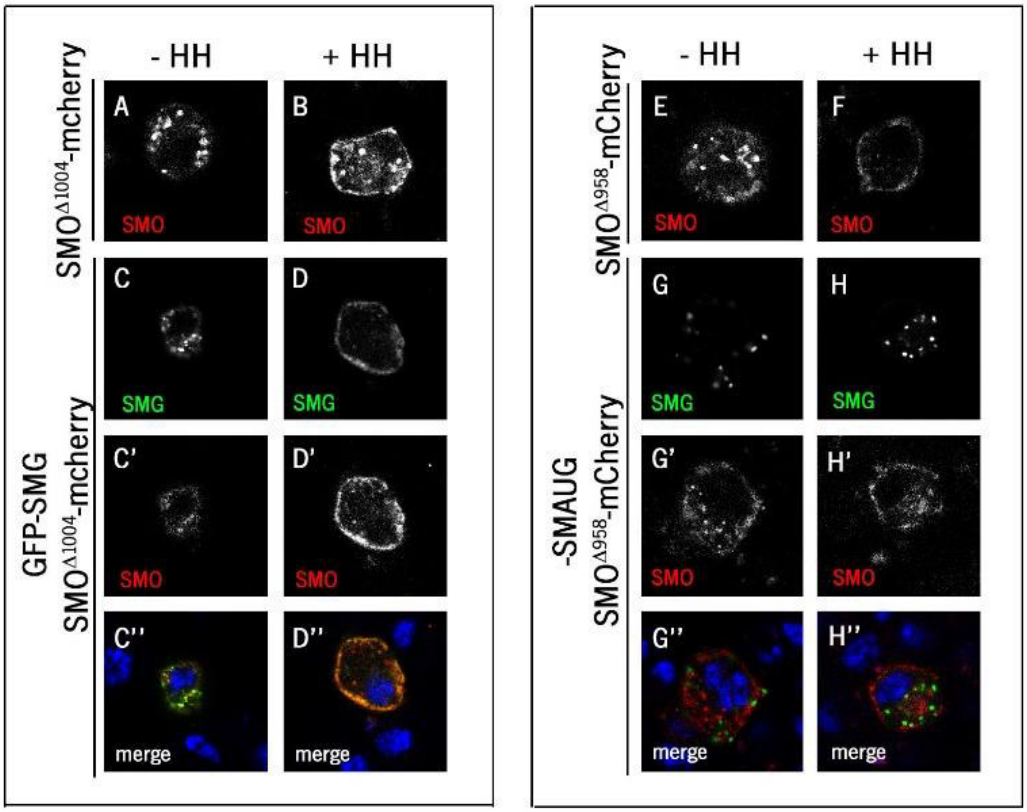

Figure 15: Subcellular distribution of SMOΔ958-mCherry, SMOΔ1004-mCherry and GFP-SMAUG in presence or absence of HH.

Cl8 cells expressing SMOΔ1004-mCherry (A, B, C' and D') or SMOΔ958-mCherry (E, F, G' and H') and GFP-SMAUG (C, D, G and H) alone (A, B, E and F) or together (C-D, G-H), with (+) or without HH (-), as indicated. Merge images are shown in C'', D'', G'' and H''.

In conclusion, the interaction between SMO-mCherry and GFP-SMAUG is required for their co-localisation, both in presence and absence of HH.

B. SMO interacts with SMAUG in a phosphorylation-dependent manner

Previous results in the lab have brought evidence that SMAUG interacted with SMO in absence and presence of HH. However, careful observation of the forms of SMO that were co-immunoprecipitated with SMAUG indicated that only the non-hyperphosphorylated forms of SMO interacted with SMAUG, but not the hyper-phosphorylated form.

My first goal was to reproduce these observations. For that purpose, I co-transfected Cl8 cells with SMO WT-HA and Myc-SMAUG, with or without HH. I then performed the Co-IP assay: I

immuno-precipitated Myc-SMAUG, and analysed the presence of the different forms of SMO WT-HA in the input (prior to the IP, Inp), the immunoprecipitated fraction (IP) and the supernatant (Sup) by Western blotting. To better compare them, I loaded these three fractions next to each other.

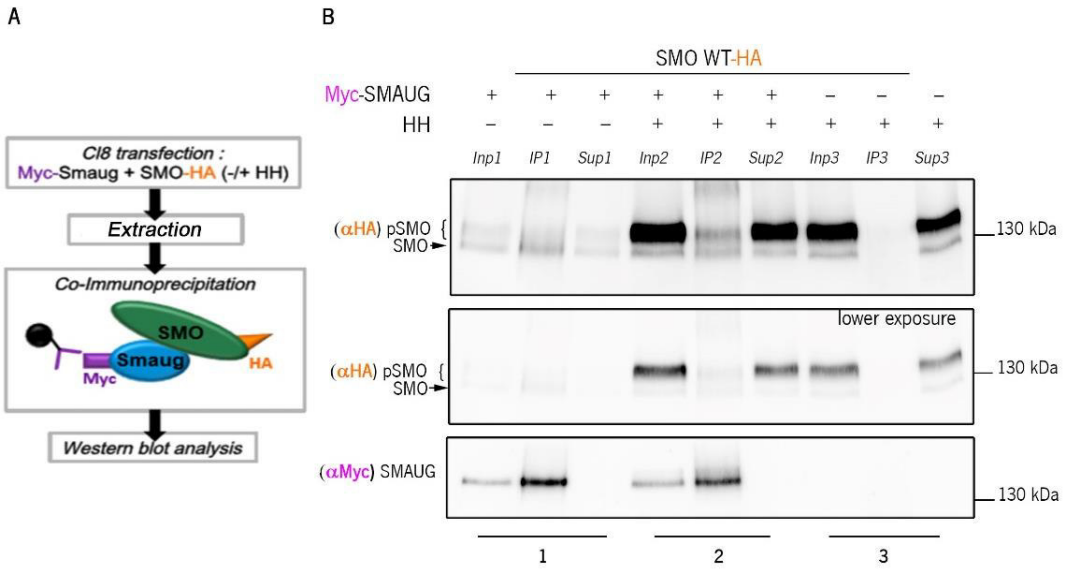

Figure 16: SMO and SMAUG co-immunoprecipitate in absence and presence of HH, however the interaction is lost when SMO is hyperphosphorylated in presence of HH.

(A) Schematic outline of the Co-IP assay main steps: Cl8 cells transiently co-transfected with SMO WT, fused to HA at its C-terminus, with (1, 2) or without (3) SMAUG fused to Myc, at its N-terminus, with (+) and without HH (-). Cell extracts were immunoprecipiated with anti-Myc antibody before Western blot analysis. (B) Immunodetection of SMO WT-HA (with an antibody against HA) and Myc-SMAUG (with an antibody against Myc) in the immunoprecipitated fraction (IP)) and in total protein extracts before (Input (Inp)) or after (Supernatant (Sup)) immunoprecipitation, with ("+") or without ("-") HH. Note that, SMO WT-HA is not immunoprecipitated in absence of Myc-SMAUG, which indicates that the interaction between SMO WT-HA and Myc-SMAUG is specific. Here and in the following figures, the molecular weights are indicated on the right, the arrowheads indicate non-phosphorylated SMO and the brackets indicate the phosphorylated forms of SMO (pSMO).

In absence of HH, SMO WT-HA is mainly non-phosphorylated with some weakly phosphorylated form *Note that, here there is some weakly phosphorylated SMO WT-HA in absence of HH, as evidenced by the phosphorylation shift* (Fig. 16 B, *Inp1*). Such low

phosphorylation is usually absent without HH. It may reflect basal levels of HH signalling possibly due traces of HH in the cell medium. Only the less phosphorylated forms are present in *IP1* (Fig. 16B, *IP1*) and both forms were still present in the *Sup.* In response to HH, SMO-HA phosphorylation levels were increased and most SMO-HA proteins were highly phosphorylated (Fig. 16B, *Inp2*). Strikingly, only the lower band, which contained non- and intermediate phosphorylated forms of SMO WT-HA, was found in the immunoprecipitated fraction (Fig 16B, *IP2*) whereas the hyperphosphorylated form of SMO remained in the supernatant (Fig. 16B, *Sup2*).

In summary, I have confirmed that i) Myc-SMAUG interacts with SMO WT-HA in presence and absence of HH and ii) that this interaction is regulated by high levels of SMO WT-HA phosphorylation, since its hyperphosphorylated form does not interact with Myc-SMAUG.

1. Identification of the phosphosites of SMO which phosphorylation prevents interaction with SMAUG

Following the confirmation of these observations, I became interested in characterising the modification of SMO that precludes this interaction. As this modification was likely to be a phosphorylation, I wanted to identify the residues of SMO of which phosphorylation prevents SMO interaction with SMAUG.

a) Serines and threonines within SMAUG-binding site of SMO C-terminal tail

Firstly, I focused on the SMAUG-binding site (SBS) of SMO. This region contains two serines and two threonines: S972, S989, T993 and T1003 (Fig 17. A). An attractive hypothesis was that the phosphorylation of one, or several, of these sites, may prevent SMO/SMAUG interaction, for instance, by altering the charge of the SBS.

To test this possiblity, I built a mutant of SMO with the four S/T residues within the SBS (S972, S989, T993 and T1003), as well as an adjacent T (1020), mutated to Alanine (A) to prevent their phosphorylation (Fig 17. A). I named this mutant SMO 5S/T A. I then repeated the Co-IP assay with SMO 5S/T A-HA and Myc-SMAUG, in absence and presence of HH.

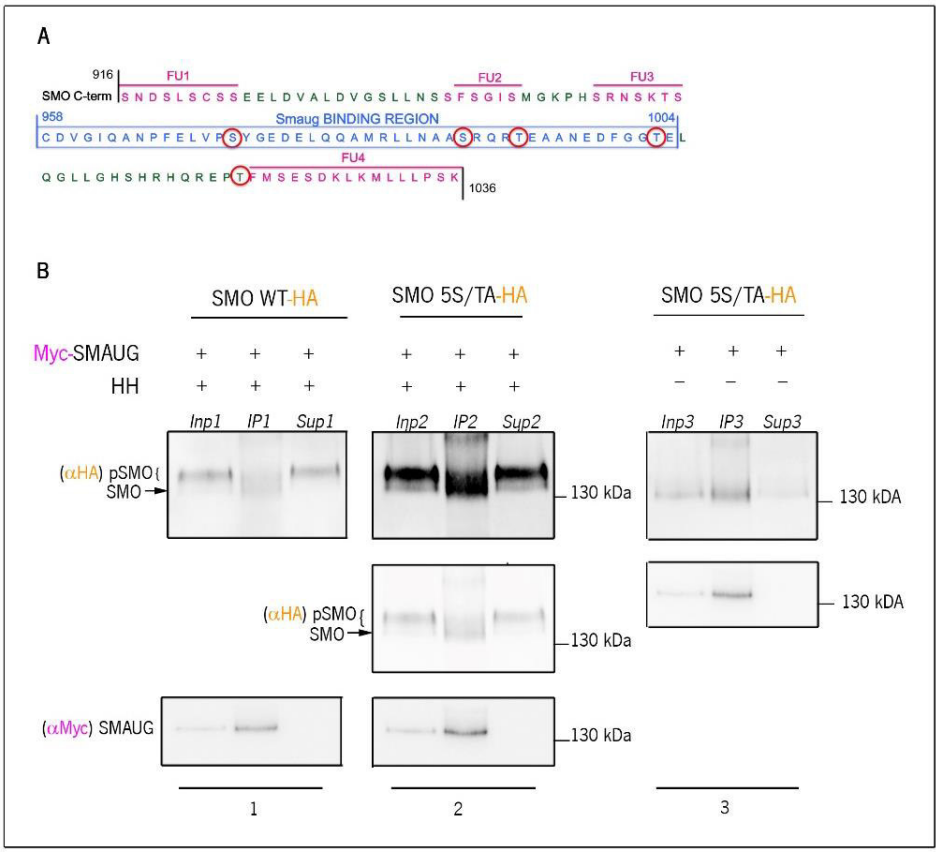

Figure 17: Co-IP of SMO 5S/TA-HA with Myc-SMAUG in presence and absence of HH

(A) Schematic representation of a region of SMO C-tail that contains the SBS in between the Fu phosphorylation clusters. The S and T encircled in red were mutated to Alanine (SMO 5S/TA). (B) Co-IP of SMO WT-HA (1) or SMO 5S/TA-HA (2 and 3) with Myc-SMAUG (1-3) in extracts of transfected Cl8 cells in presence (1 and 2) or in absence of HH (3). 1 and 2 were loaded on the same gel. 3 was loaded in a different one.

Just like SMO WT-HA, the levels and phosphorylation of SMO 5S/TA-HA were increased in presence of HH (Fig. 17B), which indicates that this mutant was still hyper-phosphorylated. Moreover, here also, Myc-SMAUG interacted with non- and intermediate phosphorylated forms of SMO 5S/TA-HA (evidenced by the smear in *IP2,* Fig. 17B), but not with the hyperphosphorylated form that remained in the supernatant (Fig. 17B, *Sup2*). In parallel, I also tested other mutants of SMO in the SBS, which were mutated for only one or two of the candiates S/T SMO S972A HA, SMO S989A T993A HA and SMO T1003A HA. These mutants, however, behaved like SMO WT-HA in what concerns to their interaction with Myc-SMAUG in presence and absence of HH (data not shown).

In summary, blocking individual or collective phosphorylation of the SBS S/T residues did not allow interaction between the hyperphosphorylated form of SMO WT-HA and Myc-SMAUG. This demonstrates that the phosphorylation of these sites is not involved in the regulation of SMO/SMAUG interaction.

b) Other phosphosites in SMO C-terminal tail

A second possibility is that the blockage of the interaction could be an indirect effect of other phosphorylations of regions of the SMO C-tail. Indeed, the hyperphosphorylated state of SMO is due to multiple phosphorylation by many kinases such as PKA/CK1, Fu, Gprk2, GISH, aPKC and CKIIβ (Fig. 18A). The phosphorylation of several of these sites have been shown to change the structure of the SMO C-tail, and may thus indirectly control the accessibility of the SSB.

The involvement of the PKA/CK1 and the FU phosphorylation clusters has been tested in the lab, prior to my arrival, and it led to the conclusion that they do not regulate the interaction between SMO and SMAUG. I made a bibliographic study on the phosphorylation of SMO. I thus identified the different mutants that I could employ to test this possibility (see Materials and Method, Table 2) and I obtained them from the relevant labs.

c) Gprk2, aPKC and GISH phosphosites

I first tested a mutant in which 18 S/T residues that have been shown to be phosphorylated by Gprk2, aPKC and Gilsh, were replaced together by A: SMO c14A. This allowed me to test multiple sites at once, but I also prepared the other mutants DNA in case I would need a more refined analysis.

Originally, the SMO c14A that I received was tagged with the GFP. However, it was impossible to interpret the results of the Co-IP. This could be due to the antibody against the GFP with which there was little experience in the lab. To circumvent this problem, I decided to change tag to HA.

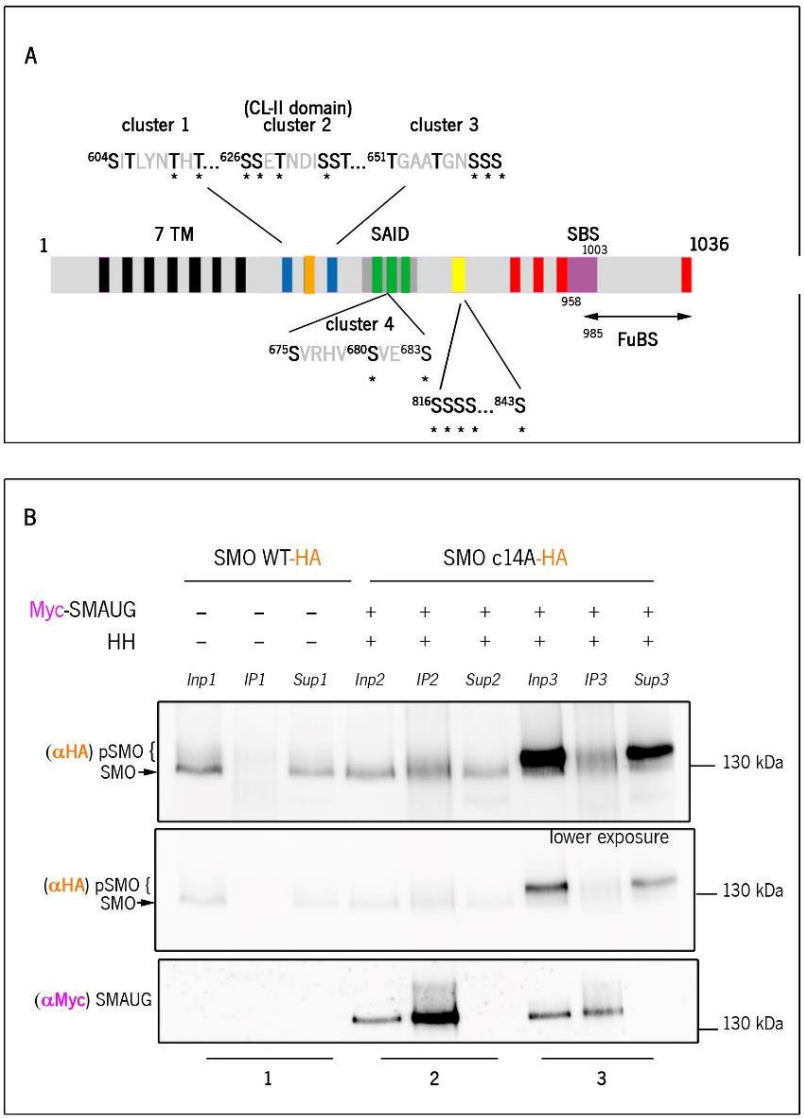

Figure 18: Co-IP of SMO c14A-HA with Myc-SMAUG in presence and absence of HH

(A) Schematic representation of SMO protein. Colourful boxes represent different kinase phosphorylation cluster: GprkII; Gish; PKA/CK1; CKIIβ; and Fu clusters. S residues 680 and 683 are phosphorylated by aPKC and CK1, respectively. S/T in clusters 1-4 (c14) are mutated to A in SMO c14A-HA. Purple box: SBS. FuBS stands for Fu Binding Site. Black boxes correspond to the seven transmembrane domains. Asterisks indicate phosphosites identified by Mass Spectrometry. (B) Immuno-detection of SMO WT-HA (1) or SMO c14A-HA (2 and 3) and Myc-SMAUG (2 and 3) in extracts of CI8 cells transiently expressing each protein with (3) or without HH (1 and 2). 1 and 2 were loaded on the same gel. 3 was loaded in a different one.

As shown in Fig. 18B, Myc-SMAUG was able to immune-precipitate SMO c14A-HA in absence of HH (*IP2*). In presence of HH, SMO c14A-HA over-accumulated and was hyper-phosphorylated, as shown by its retardation in migration (Fig. 18B, *Inp3* compared with *Inp2*). Here also, Myc-SMAUG interacted with non- and intermediate phosphorylated forms of SMO c14A-HA (Fig. 18B, smear in *IP3*), but did not interact with the hyperphosphorylated form of SMO c14A-HA. This form remained in the supernatant (Fig. 18B, *IP3* compared with *Sup3*).

I therefore concluded that the phosphorylation of the clusters 1-4 is not responsible for the blockage of the interaction between SMO c14A-HA and Myc-SMAUG.

d) CKIIβ phosphosites

Finally, I also wanted to test the CKIIβ phosphosites, which were not mutated in SMO c14A mutant. For that purpose I used a Myc-tagged mutant that I had received and in which all the five residues phosphorylated by CKIIβ are mutated to A. I named it SMO CKIISA

Since SMO CKIISA was tagged with Myc (at its N-terminus), I first analysed it by Western Blotting to confirm its expression, response to HH and correct detection (Fig. 6 A-B). At the same time, I tested other Myc-SMO mutants received from the same lab that I could have needed of for future studies. This first preliminary analysis (fig. 19A, B) revealed two things: (i) the presence of extra bands that I did not expect, and (ii) in presence of HH, a poor resolution (compared to what I usually see with SMO WT-HA) between the non- and hyperphosphorylayed forms of the Myc-SMO constructs (Fig. 19 A, B). Regarding the second observation, I decided to compare the migration of Myc-SMO WT and SMO WT-HA, in the same gel. After the transfer, I cut the membrane in two, and labelled them separately. There were striking differences between the behaviours of Myc-SMO WT and SMO WT-HA. First, Myc-SMO WT migrated at a higher position in the gel. Second, the separation between the non-phosphorylated and the hyperphosphorylated forms of Myc-SMO WT were not as well resolved as the one between the forms of SMO WT-HA. Finally, the extra bands were still present with Myc-SMO WT but absent with SMO WT-HA. (Fig. 19C, see legend for hypothesis on the possible causes of the problem).

(v)

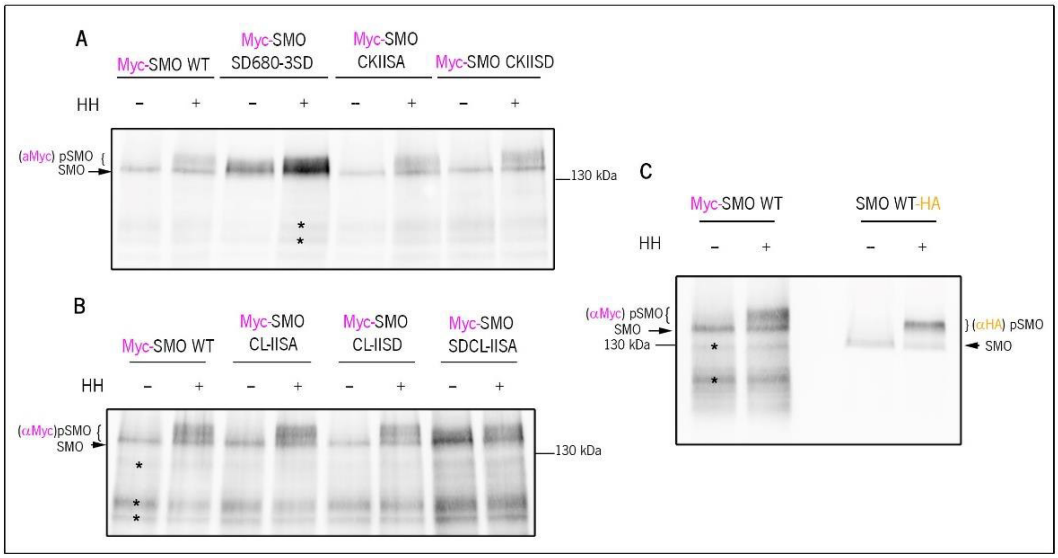

Figure 19: Expression of several Myc-SMO mutants in presence and absence of HH.

(A-C) Detection of various constructs of Myc-SMO (as indicated) by Western blot analysis (with an anti-Myc antibody) in transfected CI8 cells extracts. All the HA-SMO constructs are are phosphorylated in response to HH.

All mutants are described in the Table 2). Asterisks indicate extra bands that were not expected. The antibody used could be the cause of these extra bands. But in absence of a non-transfected control, I cannot analyse this possibility. I can say however, that I have used the same antibody, under the same conditions to detect Myc-SMAUG (see Fig. 16), and I did not observe any extra bands. Perhaps, the extra bands were truncated forms of the proteins caused by the N-terminal Myc tag. (C) There is a marked difference in migration between Myc-SMO and SMO WT-HA. The antibody cannot explain this difference, and it is unlikely that the cause of it is the difference in MW between the tags, Myc and HA.

Whatever the precise reason, since I had too little time to make new constructs, but I really wanted to have some results, I went on with the Co-IP assay. I co-transfected CI8 cells with Myc-SMO WT, Myc-SMO CKIISA and HA-SMAUG, with or without HH. However, the Co-IP was inconclusive (data not shown). The extra bands throughout each lane of the blot were many and so strong as to make it really hard to identify what was the non-phosphorylated and what was the hyperphosphorylated forms of the Myc-SMO mutants.

In conclusion, these experiments have to be repeated after changing the tag's nature and position, with a fusion of HA tag to the C-terminal part.

2. Identification the kinase responsible for the phosphorylation that prevents SMO interaction with SMAUG

At the same time that I was working on the mapping of the SMO phosphosites that regulated its interaction with SMAUG, I was also trying to identify the kinase(s) responsible for the phosphorylation that precludes the interaction between SMO and SMAUG. The strategy I used was based on the expression of shRNAs (21 nucleotides) to knockdown the expression of candidate kinases. I started with six kinases that were known to phosphorylate SMO: CK1α, GISH, CKIIβ, aPKC, PKAc1 and Gprk2

At first, I wanted to validate my strategy by analysing the impact on SMO phosphorylation of the knockdown of their respective expression. For this purpose, I transfected Cl8 cells with SMO PKASD-HA and each of the shRNAs. I then analysed SMO PKASD-HA phosphorylation by Western blotting.

I used SMO PKASD-HA which is constitutively active due to the replacement of the PKA/CKI phosphosites by aspartic acid (D) which mimicked their phosphorylation. This mutant is known to accumulate at the the plasma membrane and to be phosphorylated by the other SMO kinases, independently of HH. This latter point was used to facilitate my analysis because the gel shift associated to these phosphorylations was more reproducible that the one seen with SMOWT-HA in response to HH.

The lack of effect of the shRNA directed against the PKA was not unexpected as its S/T target sites were replaced by D. Among the other kinases, only the expression of the shRNA against Gprk2 promoted a clear reduction of the phosphorylation of SMO PKA-SD-HA (Fig. 20 (6)). However, the lack of apparent effect with the other shRNA was quite unexpected since these kinases contribute very largely to the hyperphosphorylation of SMO, and are known to phosphorylate SMO PKA-SD-HA. It is therefore possible that several of these shRNAI were inefficient. To test this possibility the *mRNA* levels of each kinase should be assessed with RT-qPCR. Note also that the shift promoted by the phosphorylation of SMO was not very important in this experiment, which may mask a weak change in the extent of the phosphorylation of SMO PKA-SD-HA.

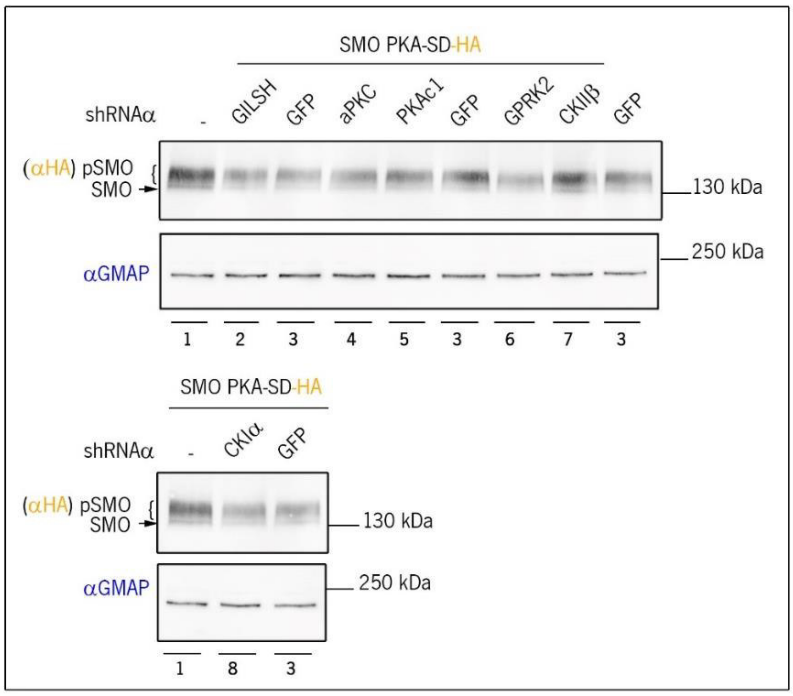

Figure 20: Validation of shRNA targeting specific kinases.

Cl8 cells were transiently co-transfected with SMO PKA-SD HA and shRNA against GISH (2), aPKC (4), PKAc1 (5), Gprk2 (6), CKIIβ (7) or CKIα (8), in absence of HH. shRNA against GFP (3) was used as control for RNAi specificity. Gmap was used as a loading control.

C. Exploring the role of SMAUG in the HH signalling pathway

Previous data based on gain-of-function studies, suggests that SMAUG is a positive regulator of the HH pathway. Indeed, overexpression of SMAUG in wildtype wing imaginal discs promotes an increase of the accumulation of SMO and of the expression of the *dpp* target gene. On the other hand, *smaug* null mutants (in which no SMAUG is expressed) have no apparent effect on the HH signalling, based on the follow-up of several HH target genes and of the wing phenotype. A recent unpublished in silico analysis has revealed that mRNAs of both positive or negative regulators of the HH pathway contain motifs that can be recognized by SMAUG, it is possible that the loss of SMAUG has multiple opposite effects that would supress each other. If the case, a partial decrease of SMAUG levels might affect some targets more than others and have some effect on HH signalling.

1. SMAUG loss or depletion has no obvious effect on HH signalling in a wild type background

My first objective was to study the effects of a reduction of *smaug* expression by RNA interference (RNAi). I used a transgenic drosophila strain that was obtained during my internship by the insertion of a construct that allowed the expression of a shRNA (21 nucleotides) directed against the sequence of SMAUG between the two SSRs (Fig. 10).

smaug-RNAi was under the control of a sequence (UAS) that could bind the yeast transcriptional activator factor Gal4. As comparing discs from different genotypes is always difficult if the effects are subtle, I drove the expression of *smaug-RNAi* by crossing the *smaug-RNAi* flies with a transgenic line that expressed the Gal4 transcription factor, but only in the dorsal half of the wing disc. This allowed me to use the ventral part as an internal control. After dissection of the discs, I immunolabelled them to detect COL and PTC. However, I saw no differences between the D and V regions. Note that I tested two independent insertions (at the same locus) of the *smaug* RNAi transgene that were available.

2. SMAUG depletion seems to enhance the patterning defects caused by *fu* loss-of-function

Another possibility was that *smaug* may ensure strong robustness of the pathway, but due to some functional redundancy, may not be essential. This is, for instance, the case for Suppressor of fused which encodes an antagonist of FU, and which loss of function has no visible effects unless the *fu* gene is mutated. I therefore tested the effects of the deregulation of *smaug* in a sensitized genetic background in which HH signalling was already reduced, due to a mutation in the *fu* gene.

For that purpose, I crossed a fly line harbouring the fu^{1} mutation along with the wing specific Gal4 driver called MS1096 with a line that carried a *UAS-smaug*-RNAi transgene. As above, I used two lines, called **M1M** and **M2M** which carry exactly the same *UAS-smaug RNAi* transgene, inserted in the same locus of chromosome 3.

Whatever, the line, the cross was established in such a way that I could compare *MS1096* fu^{1} hemizygous males in presence or in absence of a *smaug*-RNAi trasngene. The fu^{1} mutation leads to a change in the wing vein patterning with a narrowing of the space between LV 3 and 4

(see Fig. 21 A and D). At 25°C, expression of the *smaug-RNAi (M1M)* led to an aggravation of the fu1 phenotype, which translated into extra-vein tissue, some anastomosis, and narrowing of the space between LV3 and LV4 (Fig. 21 (A) E and F). To better quantify these effects, I scored the wings according to the severity of the phenotype into "weak", "medium" and strong" classes. As seen in Fig. 21 B, expression of this transgene led to a statistically significant increase of the strong phenotype associated to a decrease of the weaker one. Surprisingly, although the two lines were supposed to be equivalent, I saw no effect with the *M2M* line. As these first crosses were done with fly stocks that were directly issued from the first generation of transgenic larvae, (that were heterozygous for the transgene, and I had to check the presence of at least one copy of the transgene, which I could do thanks to an eye marker colour), it is possible that the *smaug-RNAi M2M* transgene had been absent in the progeny.

During the time of this first experiment, stocks were established using the two transgenes that were now balanced with the balancer of the chromosome III (TM3sb). I then repeated the crosses with the *fu1, MS1096* and compared again the *fu1, MS1096* and *fu1, MS1096; smaug-RNAi* males. However this time, I did not observe an aggravation of the *fu*[1] phenotype, whatever the *smaug*-RNAi insertion that I used. I repeated these crosses and the results were the same as the ones obtained for the second cross.

I did not verify whether or not the RNAi is really downregulating *smaug* expression. To validate my approach, I should have analysed the levels of SMAUG protein in third instar wing imaginal discs, and compared the results with discs that did not express the RNAi.

The fact that the *UAS-smaug-RNAi* line had been crossed with a balancer line, may have affected the transgene expression. I cannot test this hypothesis, however, since we did not keep the non-balanced line that I had first used.

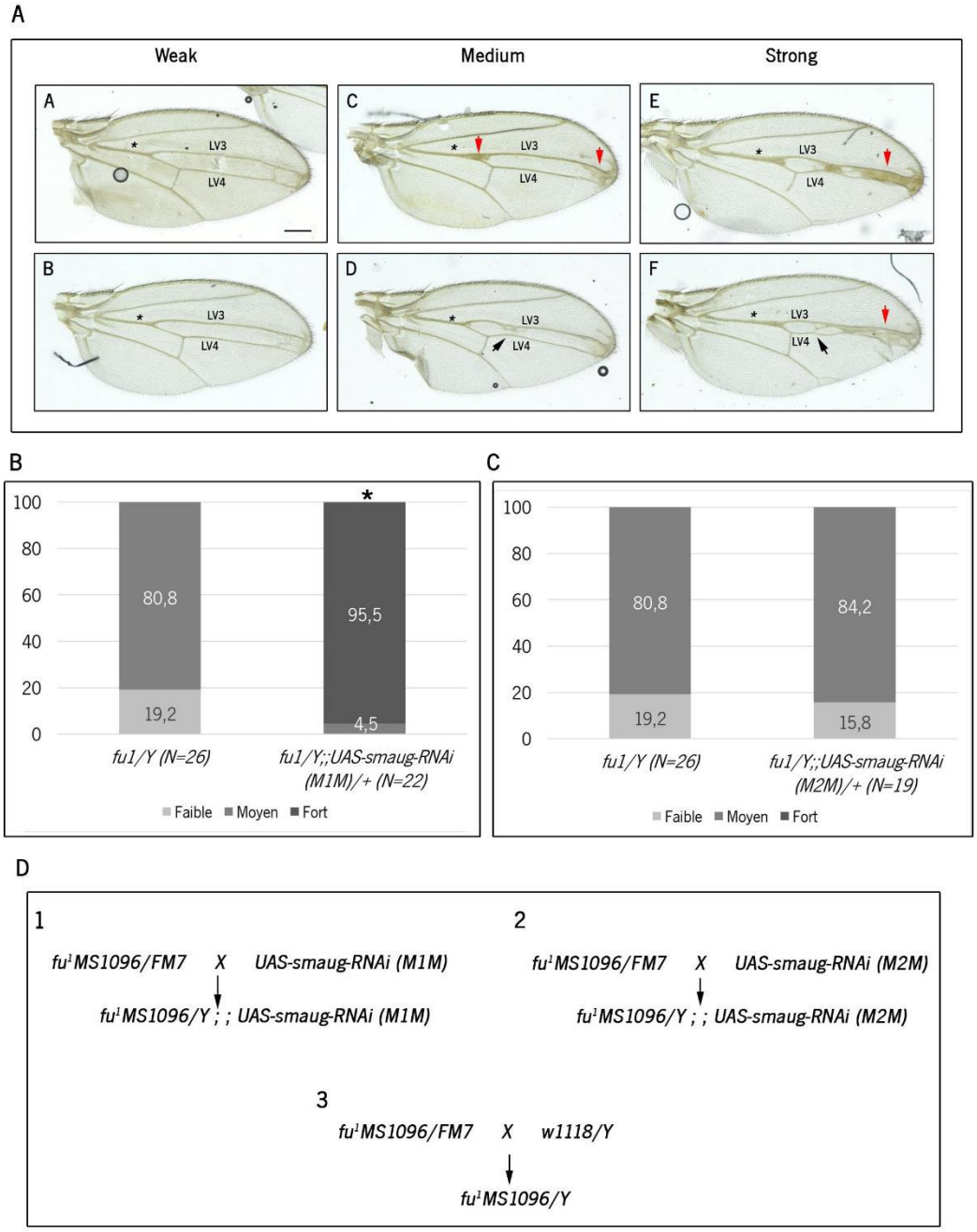

Figure 21: Genetic interaction between the Fu1 mutant and the decrease in SMAUG activity.

(A)Examples of fu¹ phenotypes observed during wing analysis. The weak phenotype is characterised by fusion of proximal region of LV3 and 4, and weak fusion of the distal extremity. In the medium phenotype, an aggravation of both proximal and distal fusion, some extra-vein tissue and anastomosis is observed. The strong phenotype is characterized by a lot of extra vein tissue and anastomosis. Black arrowhead – anastomosis; Red arrowhead – distal fusion; Asterisks – proximal fusion. Images were acquired 150x magnification. Scale bar: 500 µm. (B), (C) Effect of smaug-RNAi on [fu¹] wing class distribution. Percent distribution of phenotypic

*classes in fu^1 males in presence of zero (fu^1) or one copy (fu^1;;smaug-RNAi (M1M)/+ or fu^1;;smaug-RNAi (M2M)/+) of smaug-RNAi. The wings were classified in "weak", "medium" and "strong" according to the LV3-V4 defects. *Fisher's statistical analysis gave a p-value of 1.02e-12 when comparing fu^1 to fu^1;;smaug-RNAi (**M1M**)/+, and a p-value of 1 when comparing fu^1 to fu^1;;smaugRNAi (**M2M**)/+. (C) Crosses performed to obtain the flies analysed. 1 and 2- Gal4, under the control of endogenous drosophila promoter MS1096, drives expression of UAS-smaug RNAi. 3 - control cross.*

3. Fu knockout

Finally, I pursue using a double mutant line that had just been established, and that carried a double mutation of *smaug* and *fu.* This line had the following genotype: ***fu^0/FM7;;$smaug^0$/TM6B***. TM6B is a balancer of the third chromosome that allowed the maintenance of the *smaug* mutation despite the fact that it led to female sterility. I observed that there was no *fu^0/y;;$smaug^0$/$smaug^0$* males in this strain, while none of these mutations alone is lethal. Such effect is called a synthetic lethal effect, and is interpreted as resulting from a genetic interaction between the *fu^0* and *$smaug^0$* mutations.

IX. Discussion

My data, based on molecular, cellular and genetic experiments, confirms and extends previous observations that were made in my lab on a relationship between the HH transducer SMO and the RNA-binding protein SMAUG in the drosophila model. I, thus, confirmed that SMO and SMAUG co-localise in presence and absence of HH, and demonstrated that this co-localisation is interaction-dependent. In addition, I also showed that the interaction between SMO and SMAUG is negatively regulated by the phosphorylation of SMO. I excluded a role of the S and T residues present in the region that binds Smaug and of most of the known phosphosites of SMO such as the ones known to be targeted by the Gprk2, aPKC, and/or GISH kinases, respectively. Finally, I also genetically analysed the interaction between *smaug* and the gene *fu*, which encodes a protein kinase that is a positive regulator of the HH pathway, and, thus, showed that a double *smaug fu* mutation leads to lethality during development.

SMO and SMAUG co-localise in an interaction-dependent manner in presence and absence of HH

Through fluorescent cell imaging in tissue cultured cells, my work shows that SMAUG and SMO co-localise in cytoplasmic foci in absence of HH, and at the plasma membrane in presence of HH. This confirms observations described in S2 cells in the lab, prior to my arrival. However, the fact the two proteins co-localise does not prove that they interact with each other, as an apparent co-localisation could be due to limited the optical resolution. Using a SMO mutant that does not interact with SMAUG, I could demonstrate that co-localisation between SMO and SMAUG, requires interaction. Is this interaction direct or indirect via a common partner? An in vitro assay based on expression of SMAUG and SMO C-tail in bacteria should carried out to answer this question.

SMAUG is found at the plasma membrane with SMO in response to HH. Does it go to the plasma membrane with SMO, or is it recruited there after SMO reaches the membrane? As the two proteins interact together in absence of HH, the first hypothesis seems to be the most likely to happen. However, time-lapse fluorescence microscopy on live cells could be performed to confirm it.

SMAUG is known to form cytoplasmic foci that contain ribonucleoprotein complexes (mRNPs), which include its target mRNA, and proteins that repress them. On the other hand SMO is a transmembrane protein present in endocytic vesicles, or at the plasma membrane. This raises several questions. Are these RNP proteins and mRNA also associated with SMO via SMAUG? And if so, are they also recruited with SMAUG at the plasma membrane by SMO in presence of HH? Are the formation, the dynamic and the composition of SMAUG-foci modified in presence of SMO alone, or with HH? Analyses from SMAUG immune-complexes in presence or in absence of SMO/HH, by Mass Spectrometry to identify the protein partners of SMAUG, and by mRNA sequencing to assess its mRNA partners, may answer these important questions.

Strinkingly, C. Arguelles and L. Bruzzone, two postgraduate students from the lab have recently shown that the activation of SMO by HH promotes the phosphorylation of SMAUG (unpublished data). The phosphosites are currently being mapped. It would be very interesting to test whether this phosphorylation of SMAUG controls its interaction with SMO and its ability to form foci

SMO/SMAUG interaction is negatively regulated by SMO phosphorylation in tissue cultured cells

SMAUG does not interact with the hyperphosphorylated form of SMO, which is promoted by HH. A plausible explanation could be that the phosphorylation of specific residues in SMO C-tail prevents its interaction with SMAUG. Note that, paradoxically SMAUG co-localizes with SMO in presence and absence of HH. This is likely due the fact that in presence of HH, a fraction of SMO undergoes only partial phosphorylation, sufficient to target SMO at the plasma membrane, but not sufficient to prevent its interaction with SMO.

Whatever, I started to search for the phosphosites that could regulate the interaction between SMO and SMAUG. I tested more than twenty S/T residues and, in the end, I was able to rule out an implication of the S/T residues in the SMAUG-binding region, as well as of many well-characterised phosphosites, namely Gprk2, aPKC and GISH phosphosites(Baez & Boccaccio 2005). Previous data obtained in the lab also showed that the phosphorylation of the PKA/CK1 and FU clusters was not involved. It is however possible that combined phosphorylation of these different sites is required to prevent SMO/SMAUG interaction. Alternatively, the answer may be within the more than 20 S/T residues in the C-tail that remain to be tested, or in the intracellular loops that connect its seven transmembrane domains.

A second hypothesis is that another type of post-translational modification could be involved, that would occur when SMO is hyperphosphorylated, but not be due to this hyperphosphorylation. A recent study demonstrates that SMO undergoes sumoylation in response to HH (Ma et al. 2016). This sumoylation appears to act in parallel with the hyperphosphorylation to promote SMO accumulation levels and activity. It would be interesting to analyse the interaction with SMAUG of a form of SMO in which SMO sumoylation is prevented through mutation of the Lysine K851, to which the SUMO peptide is linked.

Another cause for the loss of SMO/SMAUG interaction could be that a protein or protein complex may interact with the hyperphosphorylated form of SMO, and, in this way, displace or compete with SMAUG. Notably, highly activated SMO is known to interact and to recruit at the plasma membrane both COS2 and FU. The FU-binding site overlaps with the SMAUG-binding site for around twenty amino acid residues. Binding of one or both of these proteins could, thus, prevent the interaction between SMO and SMAUG. However, previous data in the

lab suggest that co-expression of COS2 and FU with SMO and SMAUG did not affect their interaction. In any case, many proteins have been identified by a two-hybrid screen to interact with SMO, and one of these proteins might regulate the interaction of SMO with SMAUG.

Identification of the kinase involved in the phosphorylation that prevents SMO/SMAUG interaction

Considering the possibility that phosphorylation was directly responsible for loss of SMO/SMAUG interaction, it is also interesting to identify the kinase involved. For that purpose, I have started to downregulate (by shRNA) the expression of six kinases known to target SMO. However, with the exception of Gprk2, I had no visible reduction of phosphorylation of SMO PKA-SD with the other kinases. It could be that the shRNA does not work and RT-qPCR should be performed to assess the levels of mRNA of each kinase. If this is the case, I should test other shRNA constructs. Or, perhaps, there is an effect, but I cannot detect it because it is not strong enough to reduce the electrophoretic mobility of the phosphorylated forms of SMO. If the case, the conditions of the experiment need to be optimised.

Whatever, the marked effect of downregulation of Gprk2 expression is quite surprising, since my results also show that none of the described Gprk2 phosphosites seems to regulate the SMO/SMAUG interaction. It is possible, therefore, that novel sites targeted by Gprk2, but that have yet to be identified, are involved.

A mass spectrometry analysis of Smaug immunocomplexes with or without SMO/HH was recently performed by L. Bruzzone, a doctorate in the lab (unpublished data). It led to the identification of ten kinases that were complexed with SMAUG in both conditions. Five of them are described in the literature to be involved in the HH pathway, and five were unexpected. From the latter, one was significantly more abundant in presence of SMO/HH. This kinase may be a novel kinase in the HH pathway, and could be responsible for the phosphorylation that prevents SMO/SMAUG interaction.

Genetic interaction between *smaug* and *fu*

In a wildtype context, the downregulation of *smaug* expression by RNA interference has no detectable effect on wing morphology, nor on the expression of HH target genes, or SMO accumulation levels in wing imaginal discs. My initial data revealed, however that it had an effect in a *genetically sensitized* context, leading to an aggravation of fu^{1} phenotype, in the wing disc.

This corroborates other information obtained in the lab that shows that SMAUG may positively regulate the HH pathway. However, I was unable to reproduce these results. The interpretation of this variability will require to check (by PCR) that the *smaug*-RNAi transgenes were not lost. Another possibility is that the effects studied might be sensitive to the genetic background

During my stay in the lab, a *fu^{o}/y;;smaug^{o}/smaug^{o}* line was establish, and I used it to further explore SMAUG relationship with HH pathway. Strikingly, there are no *fu^{o}/y;;smaug^{o}/smaug^{o}* adult male or 3rd instar male larvae, which is probably indicative of synthetic lethality. To better characterize this phenomenon, it will be necessary to determine at which developmental point, and with which terminal phenotype the larvae or embryo dies. This could be performed by aligning freshly laid embryos, and following their developmental progress throughout time.

Model of the general role of SMO/SMAUG interaction in the HH pathway

Taking into account what is known on SMAUG and our present data on SMAUG and SMO, the following model could be proposed: in absence of HH, SMAUG may repress the translation or downregulate the levels of a (or several) mRNA encoding a positive regulator of the HH pathway. SMO activation by HH would lead to SMAUG phosphorylation, which would induce the release of the trapped mRNA(s) from the SMAUG-foci and promote its (or their) translation (Fig, 22). Finally very high levels of HH would lead to the dissociation of SMAUG/SMO complex via the hyperphosphorylation of SMO. In such model, SMAUG would, thus ensure the localized expression, e. g. near the plasma membrane, of this positive regulator, in response to HH. In the absence of SMAUG, this mRNA might be translated in other localisation, leading to its loss of activity, or to its degradation. Similarly, SMAUG was shown to ensure the translation of *nanos* in the posterior pole of the embryo via its repression during its transport to this pole (Smibert et al. 1996; Smibert et al. 1999).

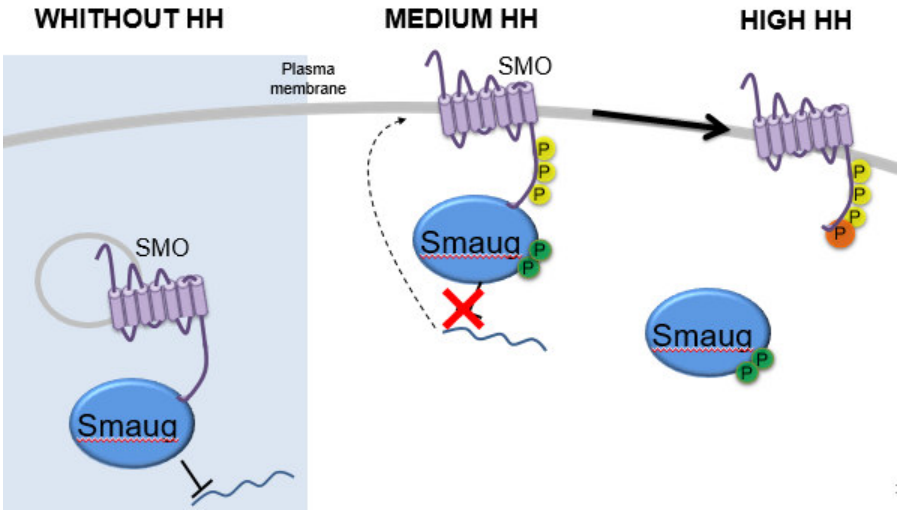

Figure 22: Model of the regulation of SMO/SMAUG interaction in presence and absence of HH

In absence of HH, SMAUG and endocytic SMO interact and co-localize; leading to the retention of repressed mRNA in SMO-bound cytoplasmic foci. In presence of HH, SMO is phosphorylated and recruits SMAUG at the plasma membrane, leading to the release of the repressed mRNA and their expression. High lelvels of HH prevent the interaction between SMO/SMAUG by promoting a hyper-phosphorylation of SMO.

Interestingly, a recent study showed that the guidance of axons growth by SHH relies on a non-canonical, SMO-dependent signalling mechanism that results in the local translation of *b-actin* mRNA in the axon growth. In this process, SHH was shown to act by promoting the dissociation of the *b-actin* mRNA from the translation repressor ZBP1, through phosphorylation of the latter (Lepelletier et al. 2017).

X. Bibliography

Alves, G. et al., 1998. Modulation of hedgehog target gene expression by the fused serine threonine kinase in wing imaginal discs. *Mechanisms of Development*, 78(1–2), pp.17–31.

Arensdorf, A.M., Marada, S. & Ogden, S.K., 2016. Smoothened Regulation: A Tale of Two Signals. *Trends in Pharmacological Sciences*, 37(1), pp.62–72. Available at: http://dx.doi.org/10.1016/j.tips.2015.09.001.

Baez, M. V. & Boccaccio, G.L., 2005. Mammalian smaug is a translational repressor that forms cytoplasmic foci similar to stress granules. *Journal of Biological Chemistry*, 280(52), pp.43131–43140.

Basler, K. & Struhl, G., 1994. Compartment boundaries and the control of Drosophila limb pattern by hedgehog protein. *Nature*, 368, pp.208–214.

Benoit, B. et al., 2009. An essential role for the RNA-binding protein Smaug during the Drosophila maternal-to-zygotic transition. *Development*, 136(6), pp.923–932. Available at: http://dev.biologists.org/cgi/doi/10.1242/dev.031815.

Briscoe1, J. et al., 2013. The mechanisms of Hedgehog signalling and its roles in development and disease. *Nature Reviews Molecular Cell Biology*, 14(7), pp.416–429. Available at: papers2://publication/uuid/C7207B88-7748-4C53-B102-8C2741247526%5Cnhttp://www.ncbi.nlm.nih.gov/pubmed/23719536.

Chen, C.H. et al., 1999. Nuclear trafficking of Cubitus interruptus in the transcriptional regulation of Hedgehog target gene expression. *Cell*, 98(3), pp.305–316.

Chen, L. et al., 2014. Global regulation of mRNA translation and stability in the early Drosophila embryo by the Smaug RNA-binding protein. *Genome biology*, 15(1), p.R4. Available at: http://genomebiology.com/2014/15/1/R4.

Chen, Y. et al., 2010. G protein-coupled receptor kinase 2 promotes high-level Hedgehog signaling by regulating the active state of Smo through kinase-dependent and kinase-independent mechanisms in Drosophila. *Genes and Development*, 24(18), pp.2054–2067.

Chen, Y. & Jiang, J., 2013. Decoding the phosphorylation code in Hedgehog signal transduction. *Cell research*, 23(2), pp.186–200. Available at: http://www.ncbi.nlm.nih.gov/pubmed/23337587%5Cnhttp://www.pubmedcentral.nih.gov/articlerender.fcgi?artid=PMC3567827.

Claret, S., Sanial, M. & Plessis, A., 2007. Evidence for a Novel Feedback Loop in the Hedgehog Pathway Involving Smoothened and Fused. *Current Biology*, 17(15), pp.1326–1333.

Dahanukar, A., Walker, J.A. & Wharton, R.P., 1999. Smaug, a novel RNA-binding protein that operates a translational switch in Drosophila. *Molecular Cell*, 4(2), pp.209–218.

Davidson, G. et al., 2005. Casein kinase 1 gamma couples Wnt receptor activation to cytoplasmic signal transduction. *Nature*, 438(7069), pp.867–872.

Ding, X. et al., 2013. NIH Public Access. , 16(3), pp.387–393.

Duffy, J.B., 2002. GAL4 system indrosophila: A fly geneticist's swiss army knife. *Genesis*, 34(1–2), pp.1–15. Available at: http://doi.wiley.com/10.1002/gene.10150.

Fan, J., Liu, Y. & Jia, J., 2012. Hh-induced Smoothened conformational switch is mediated by differential phosphorylation at its C-terminal tail in a dose- and position-dependent manner. *Developmental Biology*, 366(2), pp.172–184. Available at: http://dx.doi.org/10.1016/j.ydbio.2012.04.007.

Farzan, S.F. et al., 2008. Costal2 Functions as a Kinesin-like Protein in the Hedgehog Signal Transduction Pathway. *Current Biology*, 18(16), pp.1215–1220.

Fernández-Alvarez, A.J. et al., 2016. Smaug variants in neural and non-neuronal cells. *Communicative and Integrative Biology*, 9(2), pp.1–8. Available at: http://dx.doi.org/10.1080/19420889.2016.1139252.

Fredriksson, R. et al., 2003. The G-protein-coupled receptors in the human genome form five main families. Phylogenetic analysis, paralogon groups, and fingerprints. *Molecular pharmacology*, 63(6), pp.1256–72.

Gault, W.J. et al., 2012. Drosophila CK1-??, gilgamesh, controls PCP-mediated morphogenesis through regulation of vesicle trafficking. *Journal of Cell Biology*, 196(5), pp.605–621.

Hartl, T.A. & Scott, M.P., 2014. Wing tips: The wing disc as a platform for studying Hedgehog signaling. *Methods*, 68(1), pp.199–206.

Hsia, E.Y.C., Gui, Y. & Zheng, X., 2015. Regulation of Hedgehog signaling by ubiquitination. *Frontiers in biology*, 10(3), pp.203–220. Available at: http://www.pubmedcentral.nih.gov/articlerender.fcgi?artid=4564008&tool=pmcentrez&rendertype=abstract.

Hummel, T. et al., 2002. Temporal control of glial cell migration in the Drosophila eye requires gilgamesh, hedgehog, and eye specification genes. *Neuron*, 33(2), pp.193–203.

Ingham, P.W. et al., 2001. Hedgehog signaling in animal development : paradigms and principles Hedgehog signaling in animal development : paradigms and principles. *Genes and Development*, 15(23), pp.3059–3087.

Ingham, P.W., Nakano, Y. & Seger, C., 2011. Mechanisms and functions of Hedgehog signalling across the metazoa. *Nature reviews. Genetics*, 12(6), pp.393–406. Available at: http://dx.doi.org/10.1038/nrg2984.

Jia, H. et al., 2009. PP4 and PP2A regulate Hedgehog signaling by controlling Smo and Ci phosphorylation. *Development (Cambridge, England)*, 136, pp.307–316.

Jia, J., Tong, C. & Jiang, J., 2003. Smoothened transduces Hedgehog signal by physically interacting with Costal2/Fused complex through its C-terminal tail. *Genes and Development*, 17(21), pp.2709–2720.

Jiang, J. & Hui, C.-C., 2008. Hedgehog signaling in development and cancer. *Developmental cell*, 15(6), pp.801–812. Available at: papers2://publication/uuid/D836100E-0C44-4A8B-8E74-0BFC0BD90E59%5Cnhttp://www.ncbi.nlm.nih.gov/pubmed/19081070%5Cnpapers2://publication/doi/10.1016/j.devcel.2008.11.010.

Jiang, K. et al., 2014. Hedgehog-regulated atypical PKC promotes phosphorylation and activation of Smoothened and Cubitus interruptus in Drosophila. *Proceedings of the National Academy of Sciences of the United States of America*, 111(45), pp.E4842-50. Available at: http://eutils.ncbi.nlm.nih.gov/entrez/eutils/elink.fcgi?dbfrom=pubmed&id=25349414&retmode=ref&cmd=prlinks%5Cnpapers2://publication/doi/10.1073/pnas.1417147111.

Jiang, K. et al., 2016. PI(4)P Promotes Phosphorylation and Conformational Change of Smoothened through Interaction with Its C-terminal Tail. *PLoS Biology*, 14(2), pp.1–26.

Jiang, K. & Jia, J., 2015. Smoothened regulation in response to Hedgehog stimulation. *Frontiers in biology*, 10(6), pp.475–486. Available at: http://www.ncbi.nlm.nih.gov/pmc/articles/PMC4787298/.

Knippschild, U. et al., 2005. The casein kinase 1 family: Participation in multiple cellular processes in eukaryotes. *Cellular Signalling*, 17(6), pp.675–689.

Kuzhandaivel, A. et al., 2014. Cilia-Mediated Hedgehog Signaling in Drosophila. *Cell Reports*, 7(3), pp.672–680. Available at: http://dx.doi.org/10.1016/j.celrep.2014.03.052.

Lepelletier, L. et al., 2017. Sonic Hedgehog Guides Axons via Zipcode Binding Protein 1-Mediated Local Translation. *The Journal of Neuroscience*, 37(7), p.1685 LP-1695. Available at: http://www.jneurosci.org/content/37/7/1685.abstract.

Li, S. et al., 2012. Hedgehog-regulated ubiquitination controls smoothened trafficking and cell surface expression in Drosophila. *PLoS Biology*, 10(1).

Li, S. et al., 2016. Regulation of Smoothened Phosphorylation and High-Level Hedgehog Signaling Activity by a Plasma Membrane Associated Kinase. , pp.1–24.

Liu, Y. et al., 2007. Fused-Costal2 protein complex regulates Hedgehog-induced Smo phosphorylation and cell-surface accumulation. *Genes and Development*, 21(15), pp.1949–1963.

Lum, L. et al., 2003. Hedgehog signal transduction via Smoothened association with a cytoplasmic complex scaffolded by the atypical kinesin, Costal-2. *Molecular Cell*, 12(5), pp.1261–1274.

Luo, H. et al., 2016. The Smaug RNA-Binding Protein Is Essential for microRNA Synthesis During the Drosophila Maternal-to-zygotic Transition. *G3: Genes|Genomes|Genetics*, 6(November), pp.3541–3551. Available at: http://g3journal.org/cgi/doi/10.1534/g3.116.034199.

Ma, G. et al., 2016. Regulation of Smoothened Trafficking and Hedgehog Signaling by the SUMO Pathway. *Developmental Cell*, 39(4), pp.438–451. Available at: http://dx.doi.org/10.1016/j.devcel.2016.09.014.

Maier, D. et al., 2014. A Broadly Conserved G-Protein-Coupled Receptor Kinase Phosphorylation Mechanism Controls Drosophila Smoothened Activity. *PLoS Genetics*, 10(7).

Nelson, M.R., Leidal, A.M. & Smibert, C.A., 2004. Drosophila Cup is an eIF4E-binding protein that functions in Smaug-mediated translational repression. *The EMBO Journal*, 23(1), pp.150–159. Available at: http://emboj.embopress.org/cgi/doi/10.1038/sj.emboj.7600026.

Paris, U. et al., 2016. Characterization of the interaction between the Hedgehog transducer Smoothened and the RNA-binding protein Smaug.

Pasca di Magliano, M. & Hebrok, M., 2003. Hedgehog signalling in cancer formation and maintenance. *Nature reviews. Cancer*, 3(12), pp.903–911. Available at: http://www.nature.com/doifinder/10.1038/nrc1229.

Paslay, J., Morin, J. & Harrison, R., 2010. High Throughput Screening in the Twenty-First Century. *Topics in Medicinal Chemistry*, 5(April), pp.25–83. Available at: http://link.springer.com/chapter/10.1007/7355_2009_6.

Petrova, R. & Joyner, a. L., 2014. Roles for Hedgehog signaling in adult organ homeostasis and repair. *Development*, 141(18), pp.3445–3457.

Roote, J., & Prokop, A. (2013). How to Design a Genetic Mating Scheme: A Basic Training

Package for *Drosophila* Genetics. *G3: Genes|Genomes|Genetics*, *3*(2), 353–358. http://doi.org/10.1534/g3.112.004820

Rana, R. et al., 2013. Structural insights into the role of the Smoothened cysteine-rich domain in Hedgehog signalling. *Nat Commun*, 4, p.2965. Available at: http://www.ncbi.nlm.nih.gov/pubmed/24351982.

Ranieri, N. et al., 2012. Distinct Phosphorylations on Kinesin Costal-2 Mediate Differential Hedgehog Signaling Strength. *Developmental Cell*, 22(2), pp.279–294.

Robbins, D.J. et al., 1997. Hedgehog elicits signal transduction by means of a large complex containing the kinesin-related protein costal2. *Cell*, 90(2), pp.225–234.

Ruel, L. et al., 2003. Stability and association of Smoothened, Costal2 and Fused with Cubitus interruptus are regulated by Hedgehog. *Nature cell biology*, 5(10), pp.907–13. Available at: http://www.ncbi.nlm.nih.gov/pubmed/14523402.

Sanial, M. et al., 2017. Dose-dependent transduction of Hedgehog relies on phosphorylation-based feedback between the G-protein-coupled receptor Smoothened and the kinase Fused. *Development*, 144(10), p.1841 LP-1850. Available at: http://dev.biologists.org/content/144/10/1841.abstract.

Smibert, C.A. et al., 1999. Smaug, a novel and conserved protein, contributes to repression of nanos mRNA translation in vitro. *Rna*, 5(12), pp.1535–47. Available at: http://www.pubmedcentral.nih.gov/articlerender.fcgi?artid=1369876&tool=pmcentrez&rendertype=abstract.

Smibert, C.A. et al., 1996. smaug protein represses translation of unlocalized nanos mRNA in the Drosophila embryo. *Genes and Development*, 10(20), pp.2600–2609.

Strigini, M. & Cohen, S.M., 1997. A Hedgehog activity gradient contributes to AP axial patterning of the Drosophila wing. *Development (Cambridge, England)*, 124(22), pp.4697–4705. Available at: http://eutils.ncbi.nlm.nih.gov/entrez/eutils/elink.fcgi?dbfrom=pubmed&id=9409685&retmode=ref&cmd=prlinks%5Cnpapers2://publication/uuid/8D8B92CA-DA24-4862-A008-4B5503F14F7D%5Cnpapers2://publication/uuid/8305BF34-CB15-4938-BFC1-83B3EA257F87.

Tabata, T. & Kornberg, T.B., 1994. Hedgehog is a signaling protein with a key role in patterning Drosophila imaginal discs. *Cell*, 76(1), pp.89–102.

Taipale, J. & Beachy, P. a, 2001. The Hedgehog and Wnt signalling pathways in cancer. *Nature*,

411(6835), pp.349–54. Available at: http://www.ncbi.nlm.nih.gov/pubmed/11357142.

Vervoort, M. et al., 1999. The COE transcription factor Collier is a mediator of short-range Hedgehog-induced patterning of the Drosophila wing. *Current Biology*, 9(12), pp.632–639.

Wang, G., Wang, B. & Jiang, J., 1999. Protein kinase A antagonizes Hedgehog signaling by regulating both the activator and repressor forms of Cubitus interruptus. *Genes and Development*, 13(21), pp.2828–2837.

Xia, R. et al., 2012. USP8 promotes smoothened signaling by preventing its ubiquitination and changing its subcellular localization. *PLoS Biology*, 10(1).

Yang-zhou, D. et al., 2012. NIH Public Access. , 8(5), pp.405–407.

Zadorozny, E. V., Little, J.C. & Kalderon, D., 2015. Contributions of Costal 2-Fused interactions to Hedgehog signaling in Drosophila. *Development*, 142(5), pp.931–942. Available at: http://dev.biologists.org/cgi/doi/10.1242/dev.112904.

Zhang, C. et al., 2004. Extensive phosphorylation of Smoothened in Hedgehog pathway activation. *Proceedings of the National Academy of Sciences of the United States of America*, 101(52), pp.17900–17907.

Zhang, J. et al., 2017. SUMO regulates the activity of Smoothened and Costal-2 in Drosophila Hedgehog signaling. *Scientific Reports*, 7(November 2016), p.42749. Available at: http://www.nature.com/articles/srep42749.

Zhao, Y., Tong, C. & Jiang, J., 2007. Hedgehog regulates smoothened activity by inducing a conformational switch. *Nature*, 450(7167), pp.252–258.

Zheng, X. et al., 2010. Genetic and biochemical definition of the Hedgehog receptor. *Genes and Development*, 24(1), pp.57–71.